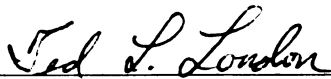THESIS

This is to certify that the

thesis entitled

WATER TRANSPORT DUE TO CAPILLARY PHENOMENA
OVER AN IMPERMEABLE BARRIER IN UNSATURATED SAND

presented by

GEOFFREY STEPHEN SALTHOUSE

has been accepted towards fulfillment
of the requirements for

_____M.S._____degree in _Agricultural_ Engineering

Ted L. London

Major professor

Date _16 October 1997_

PLACE IN RETURN BOX
to remove this checkout from your record.
TO AVOID FINES return on or before date due.

DATE DUE	DATE DUE	DATE DUE
JUL 07 1999		

WATER TRANSPORT DUE TO CAPILLARY PHENOMENA
OVER AN IMPERMEABLE BARRIER IN UNSATURATED SAND

By

Geoffrey Stephen Salthouse

A THESIS

Submitted to
Michigan State University
in partial fulfillment of the requirements
for the degree of

MASTER OF SCIENCE

Department of Agricultural Engineering

1997

ABSTRACT

WATER TRANSPORT DUE TO CAPILLARY PHENOMENA OVER AN IMPERMEABLE BARRIER IN UNSATURATED SAND

By

Geoffrey Stephen Salthouse

Capillary rise is an important mechanism in the movement of liquid through unsaturated porous media. Wastewater treatment systems can utilize this process to provide aerobic conditions while transporting the effluent to subsequent treatment or final disposal. Experiments were conducted to investigate the influence of the effective size and uniformity of sand media on capillary siphoning, defined as the transport of water by capillarity over an impermeable barrier.

U-shaped siphon tubes were filled with graded sand media of different effective sizes (0.1, 0.2 and 0.4 mm) and different uniformity coefficients (1.5, 2.5 and 4.5), capped with porous endcaps and inverted so that one leg could saturate in water. The capillary rise distance from the saturation level to the tube invert was varied stepwise to achieve steady state flow through the siphon at rise distances ranging from 2 to 10 cm. Siphon outflow was measured before the rise distance was incrementally increased.

Maximum capillary flux of 15.5 cm/hr was delivered by the 0.2 mm effective size media at a rise distance of 5 cm. Minimum flux of 0.2 cm/hr was delivered by the 0.4 mm media at 10 cm capillary rise. Media uniformity results indicate that a wide range of particle sizes may provide less capillary transport capacity under certain conditions. Further research into the influence of media uniformity on capillary siphoning is needed.

To my parents, Arlen Ross and Patricia May Salthouse, for their
ever-present and unconditional support, and who have taught me the value of
perseverance in task, and dedication to purpose. I would also like to commemorate this
work to Audrey Krajkovich who continues to be of particular inspiration.

"The knowledge of man is as the waters,
some descending from above,
and some springing from beneath."

-Francis Bacon

ACKNOWLEDGEMENTS

TABLE OF CONTENTS

LIST OF TABLES

LIST OF FIGURES

LIST OF SYMBOLS

Symbol	Description	Dimension
A	Area	$[L^2]$
$C(\psi)$	Specific moisture capacity	$[L^{-1}]$
d	Maximum particle dimension	$[L]$
D	Diffusivity	$[L^2T]$
D_{10}	Media effective size (10% finer than dimension)	$[L]$
D_{60}	60% finer than dimension	$[L]$
e	Void ratio	$[1]$
E	Pore formation factor	$[1]$
f	Water-filled porosity	$[1]$
F	Body forces	$[MLT^{-2}]$
g	Acceleration due to gravity	$[MLT^{-2}]$
G	Pore shape factor	$[1]$
h	Distance above datum	$[L]$
h_c	Capillary pressure head	$[L]$
H	Pressure head	$[L]$
H_w	Difference in free-water surface elevations	$[L]$
k	Permeability	$[L^2]$
K	Saturated hydraulic conductivity	$[LT^{-1}]$
$K(\theta)$	Unsaturated hydraulic conductivity (moisture)	$[LT^{-1}]$
$K(\psi)$	Unsaturated hydraulic conductivity (tension)	$[LT^{-1}]$
L	Distance	$[L]$
p	Pressure	$[ML^{-1}T^{-2}]$
p_0	Atmospheric pressure	$[ML^{-1}T^{-2}]$

p_b	Bubbling (air-entry) pressure	$[ML^{-1}T^{-2}]$
p_c	Capillary pressure	$[ML^{-1}T^{-2}]$
p_w	Pressure in soil water	$[ML^{-1}T^{-2}]$
q	Volumetric flux	$[LT^{-1}]$
Q	Volumetric flow rate	$[L^{3}T^{-1}]$
r	Radius	$[L]$
r_e	Pore equivalent radius	$[L]$
R_e	Reynold's number	$[1]$
S_e	Effective saturation	$[1]$
S_r	Residual (irreducible) saturation point	$[1]$
t	Time	$[T]$
$T_{1.0}$	Tortuosity at saturation	$[1]$
T_{Se}	Tortuosity at effective saturation	$[1]$
T_w	Tortuosity of the wetting phase	$[1]$
U	Coefficient of uniformity	$[1]$
v_d	Specific discharge	$[LT^{-1}]$
v_m	Thickness of media perpendicular to barrier	$[L]$
v	Linear velocity	$[LT^{-1}]$
V	Mass flux	$[ML^{-2}T^{-1}]$
W	Work	$[ML^{2}T^{-2}]$
x	Horizontal space coordinate	$[1]$
y	Horizontal space coordinate	$[1]$
z	Vertical space coordinate	$[1]$
z	Capillary rise distance	$[L]$
z	Distance above free-water surface	$[L]$
α	Solid-liquid contact angle	$[°]$
ϕ	Porosity	$[1]$
ϕ_g	Gravitational potential - per unit mass	$[L^{2}T^{-2}]$
Φ	Total (hydraulic) potential - per unit mass	$[L^{2}T^{-2}]$

γ	Surface tension	[MT^{-2}]
φ	Total (hydraulic) head	[L]
λ	Pore-size distribution index	[1]
μ	Dynamic viscosity	[ML^{-1}T^{-1}]
θ	Moisture content (mass basis)	[1]
θ_0	Initial moisture content	[1]
θ_v	Volumetric water content	[1]
ρ	Fluid density	[ML^{-3}]
ρ_b	Bulk density of media	[ML^{-3}]
ψ	Matric suction (moisture potential) head	[L]
∇	Del mathematical operator	none

Chapter 1

INTRODUCTION

Water is among the most basic necessities of virtually all life on our Earth. Its specific and peculiar characteristics allow human existence to flourish as part of a complex and remarkable ecosystem. We even dare to speculate whether life could exist on distant worlds based on possible evidence of water. It lies at the base of our subsistence and our culture. Wars are fought over it; peace is made across it. It can isolate societies, and can symbolize baptism and societal introduction. It hangs above us and runs below us. And yet its simple molecular structure—two hydrogen atoms and one oxygen atom—belies the impact that decline in quality or quantity can have on our technologically complex, and yet often aloof, society.

A clean and plentiful supply of water for current and future uses is becoming more scarce as a naturally-propagated resource. Population stresses across the globe, and even in previously remote rural communities, have mandated consideration of water treatment systems and conservation programs. Large, centralized wastewater treatment plants have been marginally successful in handling increasing purification needs, but can be economically prohibitive or practically unjustifiable. Smaller scale and localized systems are receiving greater attention and support in numerous areas, although many of these

systems are still being regarded critically in the private and public arenas. This is often due to the perception of unreliability of these "alternative" systems, although improper design, installation and/or management are more frequent causes of failure than the inherent technology.

Emulating the mechanisms of the hydrologic cycle and the myriad of physical, biological and chemical processes which commune to efficiently recycle the Earth's water resources is a challenging, yet crucial task. It is imperative that scientists work to understand and apply the pathways through which water can be reclaimed and reused in order to meet the needs—let alone satisfy the demands—of an increasingly sophisticated human population. Biological systems typically are not easily characterized and reproduced, yet they often provide the most efficacious solutions and reliable schemes.

Working in consort with water to sustain life is the "living mantle" of the planet: the soil. The interaction of these two vital resources provides us with crops, protects against flooding, even moves mountains. Much has been done, particularly in the agricultural realm, to promote and actualize investigation into the static and dynamic interchange between soil as a porous media, and water as a permeating substance. From oil reserve extraction to aquifer remediation to crop subirrigation, examples of human attempts to understand and affect porous media flow mechanisms and characteristics are numerous and diverse.

The movement of water (and other fluids) through soil takes many courses as part of the hydrologic cycle. Infiltration and redistribution are two such courses which serve to transport water according to the governing laws of potential, and the natural quest for the elusive state of equilibrium. Capillary rise, or the increase in elevation due to a potential

gradient, is another unsaturated flow mechanism which been the subject of research over the years.

Some water treatment systems, such as sand filters, take advantage of unsaturated flow in order to provide an aerobic environment for the propagation of organisms beneficial to treatment. Coupled with physical and chemical processes, this biological activity can effectively provide a level of treatment which helps to ensure proper management of animal, domestic and, to some degree, commercial wastes.

One such wastewater treatment system relies upon capillary siphoning, or transport over an impermeable barrier in unsaturated media, to provide an aerobic treatment zone following anaerobic treatment. A version of the upflow filter is now commercially available and approved for use in a limited area of the United States. In order to optimize the functionality and economics of this type of system, a need was identified for research into the hydraulic characteristics of the media specified for the capillary upflow matrix of the system. This research serves as a partial response to that need.

To that end, the specific objectives of the research described herein are to:

1) Quantify the effect of capillary rise distance (2 cm $< z <$ 10 cm) on the volumetric flow rate of water over an impermeable barrier in unsaturated sand media; and

2) Study the relationship between the geometric properties (effective size and uniformity) of the transport media and the rate of capillary siphoning over an impermeable barrier in unsaturated sand.

Chapter 2

REVIEW OF THEORY AND LITERATURE

Characterization of a Porous Media Flow System

In order to understand and optimize flow through porous media, it is important to properly describe the fundamental components of the flow system. These components are 1) the media itself and 2) the fluid (or fluids) in motion through it. Complete and accurate descriptions of these parts allow for better comprehension and application of any given flow system. Additional components, such as an organic fraction, may also exist and may affect flow through the system, but these are outside the scope of this discussion.

Media

A complete discussion of fluid transport through a porous media system would be quite extensive, considering the wide range of related fields from rock bed oil extraction to crop water requirements to wastewater treatment. While some of the concepts are common to most or all situations, it would be difficult to cover all aspects of porous media flow. Therefore this discussion will be conducted within some necessary restrictions:

1) the non-solid space in the media must be interconnected and large enough to allow entry of fluid particles; and

2) the media primarily being considered will be of unconsolidated,

granular structure.

Many of the concepts related herein hold true for other types of porous media systems such as wood, textiles, building and filter materials. This is also true for other types of porous earth materials such as those where the pore space was formed by evolution of gases during crystallization, or vugular limestone where soluble constituents of the rock have been dissolved by water forming channels (Corey, 1986).

SOLID MATRIX

The portion of the media system being considered which does not allow the entry of any fluid, even under pressure, can be described as the solid fraction. The particles of this fraction constitute the solid matrix. This matrix can also be in a continuous form, such as limestone.

A comparative and descriptive measure of the material being examined is the bulk density, ρ_b. This is the ratio of the mass of dried material to the sample's total volume. In soils ρ_b can range from about 1.1 gm/cm^3 in clay soils to 1.6 gm/cm^3 for sandy soils (Hillel, 1982). Bulk density is affected by the structure of soils, or by the degree of compaction of the media.

The solid matrix can be considered to be either consolidated or unconsolidated. An example of a consolidated porous media is limestone which maintains an overall structure. Sand is an example of an unconsolidated media, where the individual particles make up the solid matrix and exert a stress on neighboring particles if an external force is applied.

Hillel (1982) defines structure as the "arrangement and organization" of particles, and describes three general categories: single-grained, massive and aggregated. Most granular media have a single-grained structure with little tendency to adhere to neighboring particles. The arrangement of these grains can vary widely, and depends upon their relative sizes and shapes as well as the way they were deposited.

Tightly packed media in large cohesive blocks are referred to as having massive structure. An example of this is dried clay. Aggregated structure results from the primary particles grouping together in "quasi-stable clods"; these clusters acquiring their own structural characteristics (Hillel, 1982). This category is considered desirable in typical agricultural applications.

Many texts are available which comprehensively cover media characteristics, particularly soils (Terzaghi and Peck, 1967; Lambe and Whitman, 1969; Hillel, 1982). This discussion focuses primarily on sand-like materials of single-grained structure.

A number of different methods have been adopted by various disciplines to describe the geometrical makeup of a given granular media sample. One method used in soil science is the statement of relative amounts of sand, silt and clay in the sample. The commonly used USDA method defines these portions as 2 mm $\geq d \geq$ 0.05 mm, 0.05 mm $> d >$ 0.002 mm, and $d \leq$ 0.002 mm respectively, where d represents the largest dimension of a particle (Hillel, 1982; Singer and Munns, 1987).

Engineers generally define unconsolidated media particles using two variables: effective size, D_{10}, and uniformity coefficient, U. The effective size is defined as the particle size for which ten percent of the total mass of the air-dried media is finer. The

uniformity is a measure of how much the particle sizes vary within a media sample. It is defined as the ratio of the D_{60} to the D_{10}, where the D_{60} defines the particle size for which sixty percent of the total mass is finer (Terzaghi and Peck, 1967).

PORE NETWORK

The pore space within any porous media is considered to be either effective or isolated. Effective pore space is interconnected and forms a continuum, or network, within the media. This includes dead-end, or blind, pores. On the other hand, some of the non-solid space within the sample is not interconnected and therefore considered to be isolated from the effective pore network. These isolated pores do not contribute to fluid transport through the media.

Pore space can exist within individual grains of a porous media (primary pore space) as well as between aggregates of the material (secondary pore space). The presence of aggregates implies some amount of particle cementation, although secondary pore space can exist without it. The total volume of pore space, relative to mass, of media with aggregated structure is typically greater than that which is not. (Corey, 1986).

Significant parameters which are used to describe the non-solid space contained within a sample of porous media are porosity, bubbling pressure, permeability, and tortuosity. Descriptions in the literature of this pore space range from idealized models of unconnected bundled tubes (Morel-Seytoux, 1969) to complex network systems (Dullien, 1972).

One of the primary descriptors of effective pore space is the porosity ϕ. Porosity can be defined as the ratio of the interconnected, non-solid volume to the total volume of the sample of media being considered. As a ratio, ϕ is dimensionless and is theoretically bounded by 0 and 1, although practical values in granular porous media range from about 0.3 to 0.6. The volumetric water content θ_v, defined as the water-filled portion of the total volume of a media system, can approach ϕ under saturated conditions. An alternate description of the void space in a media is the void ratio e which is defined as the ratio of the volume of voids to the volume of solid substance (Terzaghi and Peck, 1967).

Media with structure will have higher porosities than those without. The shape of the grains can have an effect on porosity, as plate-shaped particles could be oriented in such a way as to create porosities lower than that of spheres, although the opposite is also possible. Porosity is usually minimized for media containing grains of widely varying sizes as the smaller particles can move into the spaces between the larger particles. It is also possible for organic and mineral cementing materials (and other precipitates) to reduce porosity. This means that consolidated sandstones generally have lower porosities than unconsolidated sand. Corey (1986) gives some approximate porosities for various typical materials:

Consolidated sandstones	0.10-0.30
Uniform spheres packed to theoretical minimum porosity	0.26
Unconsolidated sands	0.39-0.40
Soils with structure	0.45-0.55

The "size" of a pore is a difficult thing to define exactly. Unlike a capillary tube, a pore typically does not have any discreet diameter or length, but rather has a variety of interconnections with other pore space through throats or constrictions (Dullien, 1972).

The average pore size of a reference volume in a sample is defined by Corey (1986) as the ratio of the porosity of the sample to its specific surface. The specific surface is defined in his text as the ratio of internal solid surface area to the total volume, although he notes that in some cases it is considered the ratio of this area to the mass of the solid. Average pore size is analogous to the concept of hydraulic radius in hydraulics in that it refers to the ratio of the volume of the pore to the surface area bounding it. Pore size is therefore associated with grain size and distribution in that smaller grains generally mean smaller pores. Porous media with structure can, however, have larger pores associated with the secondary pore space (Corey, 1986).

Malik et al. (1984) discussed the shape factor G as a means of describing a pore's geometry. These authors proposed that G could be written as

$$G = \frac{8}{f} + E$$

where f is the water-filled porosity (or effective saturation S_e) and E is their formation factor. This formation factor accounts for the tortuosity, shape and continuity of the flow pathways in the porous media, and was empirically related to the permeability k of the media as

$$E = 126 - 166280k^{\frac{1}{2}}.$$

The proposed shape factor formula is valid for a capillary tube where $f = 1$ and $E = 0$. Therefore G is equal to a value of 8 for circular, uniform diameter capillaries.

Porous media was also compared by the authors to a "group of communicant tubes" which can be characterized by an equivalent radius r_e. This parameter is defined as the radius of a capillary tube which would exhibit equivalent behavior. Transmission constants derived from the results of capillary rise experiments were used to predict the pore geometrical properties E, G and r_e (Malik et al., 1984). These predicted values for r_e were later found by Kumar and Malik (1990) to be higher and linearly related to the mean pore radius determined from soil water desorption curves. Lawrence (1977) calculated r_e from desorption curves assuming cylindrical pores and applying the classic capillary rise equation in the form

$$\rho g h = \frac{2\gamma \cos \alpha}{r_e}$$

where $\rho g h$ is the applied suction, γ is the surface tension of the fluid and α is the solid-liquid contact angle.

The breakdown of the pore space within an element into various ranges of pore size is defined as the pore-size distribution. This is somewhat related to the grain-size distribution in that generally a greater variation in grain sizes means a greater range of pore sizes. An exception can be found in the case of a sample which has been mixed to the point that the pore-size distribution is fairly uniform even with a wide grain-size distribution.

Brooks and Corey (1964) state that the pore-size distribution index λ evaluates the distribution of sizes of the flow channels within a particular porous media. They present experimental evidence that (for isotropic media) this parameter, along with the bubbling

pressure p_b, can be used to describe the functional relationships among saturation,

capillary pressure and the air and water permeabilities.

The pore-size distribution index is defined by the authors as the slope of the log-

log graph of effective saturation S_e as a function of capillary pressure head ($p_c/\rho g$). The

empirically derived equation is

$$S_e \cong \left(\frac{p_b}{p_c}\right)^\lambda$$

where p_b is the capillary pressure at which desaturation of the media begins. λ was found

to range from a value of less than 2 in media with well-developed structure (less uniform)

to values of 5 for some sands (more uniform). There is a tendency for finer materials to

have smaller values of pore-size distribution index, although thorough mixing and dense

packing can cause λ to increase. It was determined experimentally that λ varies inversely

with ϕ (Corey, 1986).

Hillel (1982) also states that the pores in coarse-textured soils are usually more

uniform in size. However, Laliberte and Brooks (1967) found that pore-size distribution is

changed only slightly over a wide range of porosities (varied by changes in bulk density)

while the hydraulic conductivity and bubbling pressure of a given media may change

several-fold over the same range.

Brooks and Corey (1964) discuss how, under certain conditions, λ and P_b can be

used to describe the requirements for similitude between any two flow systems in porous

media. Laliberte and Brooks (1967) later stated that for modeling purposes, one

requirement for similitude between model and prototype is identical values of pore-size

distribution index. The size reduction of the model is determined by the ratio of the bubbling pressures in the model and the prototype. Evidently, the bubbling pressure of the model medium may be adjusted to suit the size of the model by changing the bulk density and hence the porosity of the medium without appreciably changing the pore-size distribution index.

Bubbling pressure p_b, or air-entry pressure, has been defined by Brooks and Corey (1964) as the lowest capillary pressure at which a continuous gas phase can exist within the media. They state that the bubbling pressure is related to the maximum pore-size forming a continuous network of flow channels within the medium. They also present experimental evidence that (for isotropic media) this parameter, along with the pore-size distribution index λ, can be used to describe the functional relationships among saturation, capillary pressure and the air and water permeabilities.

Stakman (1966) used the air bubbling pressure to determine the equivalent pore diameter, from which he calculated the mean particle size of the sand separates and thereby determined the hydraulic conductivity of the sample. He compared these estimates to the values calculated from the Kozeny-Carman equation and the Brinkman formula.

Air entry into media with coarse texture is often more distinct than finer media due to the more uniform pore sizes which usually exist in the coarser media (Hillel, 1982). More rapid desaturation will occur at this critical pressure due to the large fraction of pores which begin to drain as p_b is reached.

The permeability k is the portion of the hydraulic conductivity K of a media flow system which is a factor only of the media itself, independent of the fluid properties and

the flow mechanism. Permeability is measured in darcys where one darcy is equal to a flow

rate of one cubic centimeter per second of a fluid with a viscosity of one centipoise

through a cube having sides one centimeter in length under a pressure difference of one

atmosphere. Permeability, sometimes referred to as specific, or intrinsic permeability, is

related to K as

$$K = \frac{k\rho g}{\mu}$$

where ρ is the fluid density, g is the acceleration due to gravity, and μ is the dynamic

viscosity of the fluid (Corey, 1977).

Carman (1941) speculated that media permeability could be calculated from

particle size and porosity, while more recently Malik et al. (1984) state that the intrinsic

permeability of porous media is determined by the geometrical properties of the pores,

such as equivalent radius r_e and the shape factor G. This shape factor accounts for

porosity, tortuosity, shape and continuity of conducting channels in the media.

Suter (1964) declared that the capacity of a soil to store fluid is proportional to its

porosity, but porosity has little effect upon permeability. However, the usefulness of this

storage capacity is dependent upon permeability, which in turn depends upon continuous

passageways through the media. The introduction of finer particles reduces permeability

by increasing tortuosity with minimal changes to porosity (Suter, 1964).

Fluid particles of the wetting phase must travel an increasingly tortuous path as the

media desaturates. This is because the particles can no longer travel across the center of

pore spaces where the non-wetting phase now exists. Corey (1986) determined that (for

isotropic media) the tortuosity of the wetting phase T_w is inversely proportional to effective saturation S_e as

$$\left(\frac{T_{1.0}}{T_{S_e}}\right)_w \cong S_e^{2}$$

where $T_{1.0}$ is the tortuosity of the wetting phase at saturation ($S_e = 1.0$). Effective saturation represents the fluid available above the "irreducible" or residual saturation point S_r. Below this point the moisture is considered to contribute negligibly to flow (Corey, 1986).

Fluid

The other major component of the porous media flow system, in addition to the media, is the fluid which is being transported through it. The characteristics of the flow system depend upon both the media properties and the fluid properties. The fluid can be in a liquid or a gas phase, or in a combination of these. If more than one fluid, or more than one phase of the same fluid, occupies the pore space concurrently the system is said to be unsaturated with respect to the specified fluid.

Some primary parameters of the fluid which affect its ability to move through the media system include the surface tension γ and the viscosity μ. These parameters are in turn affected by such variables as temperature and impurities in the fluid.

The molecules on the surface of a liquid experience an unbalanced force due to their attraction to molecules in the interior of the liquid. This net inward force causes a tension to be created in the surface which can be measured. The molecules in the interior are in a lower energy state than those at the surface so molecules attempt to move into the

liquid's interior. Surface tension γ is a measure of the energy required to increase the surface of the liquid, and is inversely affected by temperature. For water at 25°C, $\gamma = 7.20 \times 10^{-2}$ J/m^2.

For liquid to spread across the surface, or wet, another material a small amount of energy must be expended. Whether the liquid will wet the surface or retain its spherical shape depends on how the cohesive forces between like molecules compare to the adhesive forces between unlike molecules, such as those of a liquid and those of the surface. The liquid will wet the surface as long as the adhesive forces are sufficiently strong. Otherwise a liquid drop will be maintained on the surface.

Adding a detergent to water lowers the surface tension of the water. A decrease in surface tension corresponds to a decrease in the energy required to spread the drop into a film. Substances which reduce the surface tension of water are known as wetting agents (Petrucci, 1985).

In the area of contact between the two-fluid surface and the solid surface, the interfacial forces act along the planes of contact between the three phases. It is difficult to measure the interfacial force which exists at the solid-liquid interface, although it is important in unsaturated systems. This force controls the contact angle α of the interface between the two fluids in contact with the solid. This angle, which is measured through the denser fluid, determines which is the wetting or the non-wetting fluid (Corey, 1986). Using glass beads and water, Laroussi and De Backer (1979) measured contact angles ranging from 41° to 66° for wetting and drainage respectively, supporting results of previous work by other authors.

Wettability describes how fast a fluid will spread over a surface, and is inversely related to surface tension and viscosity (Corey, 1986). Young's equation states that for the interfacial forces to be in equilibrium,

$$\gamma_{LG} \cos \alpha + \gamma_{SL} = \gamma_{GS}$$

where the subscripts refer to the liquid-gas (LG), the solid-liquid (SL) and the gas-solid (GS) interfaces. The first term on the left side of the equation is referred to by Bear (1979) as the adhesion tension. This determines which fluid will preferentially wet the solid surface by adhering to it and spreading out over it. For $\alpha < 90°$ the denser fluid is considered to wet the solid (ie. water and air), while for $\alpha > 90°$ the denser fluid is said to be the non-wetting fluid (ie. mercury and air).

Viscosity μ is also a function of intermolecular forces of attraction. It is related to shear force and deformation rate, and can be thought of as a fluid's resistance to flow. Temperature increase will generally cause a reduction in μ as the strength of molecular forces of attraction are lowered (Petrucci, 1985). Newtonian fluids—such as air, water and oil—exhibit direct proportionality between shear stress and the velocity gradient of the fluid near the shear surface (Potter and Wiggert, 1991).

The flow mechanism which consists of two distinct fluids displacing each other without mixing is called immiscible displacement. In miscible situations there is no distinct interface between the fluids, such as fresh and salt water in an estuary, or aquifer intrusion (Freeze and Cherry, 1979). Immiscible fluids are characterized by this boundary across which discontinuities in density and pressure exist (Corey, 1986).

Transport Phenomena in Porous Media

Energy And Potential

Classical physics defines energy in two principal forms: kinetic and potential. Movement of water through unsaturated media is generally at very low velocities, and because kinetic energy varies with the square of velocity this form is generally considered to be negligible. This leaves the potential energy of the water in the media as the predominant form. The difference in this potential between two zones becomes the driving force for water movement through the media as it attempts to reach and maintain an equilibrium condition (Hillel, 1982).

Water in a porous media is different from pure, free-standing water in that it is influenced by force fields in addition to those due to body forces such as gravity. These include the attraction of the solid matrix and the effect of dissolved constituents.

TOTAL POTENTIAL

The energy state of water in soil or other porous media can be described relative to its free energy per unit mass, or potential (Hillel, 1982). It is necessary to discuss the concept of potential in order to describe flow through porous media as it is the gradient of this energy field which is the driving force for flow. This is true for both saturated and unsaturated media conditions, the difference being the individual factors which make up the total, or hydraulic, potential. This potential is of more importance as a relative measure of energy level rather than as an absolute quantity. According to the International Soil

Science Society (Aslyng, 1963 in Hillel, 1982), the formal definition of "total potential" of soil water is

> "...the amount of work that must be done per unit quantity of pure water in
>
> order to transport reversibly and isothermally an infinitesimal quantity of water
>
> from a pool of pure water at a specified elevation at atmospheric pressure to
>
> the soil water (at the point under consideration)."

In actual practice the potential is determined by measuring some other property, such as pressure or elevation, which has a known relationship to the potential.

The total potential consists of contributions from various factors, such as the gravitational potential, the matric potential, the osmotic potential and possibly others. These other factors exist under conditions which vary according to each individual case being examined, and in many cases are of negligible influence on the total potential (Klute, 1952).

In this discussion, the total potential Φ will be considered to be the sum of two components: the pressure potential ("matric" potential for unsaturated flow), ϕ_m, and the gravitational potential, ϕ_g. There may be other potentials, such as osmotic and adsorptive potentials, depending upon whether or not the pertinent force fields are present and act upon the water in the porous medium. The total water moving field is given by

$$- \nabla \Phi = -\nabla(\phi_m + \phi_g).$$

Freeze (1969) wrote that the existence of continuous saturated-unsaturated flow domains implies the existence of this potential field, with the potential quantity defined in

such a way that it is valid both above and below the water table. He referred to the quantity as the hydraulic potential

$$\Phi = gz + (p - p_0) / \rho$$

where Φ is the hydraulic (or total) potential (cm^2/sec^2), g is the acceleration due to gravity (cm/sec^2), z is the elevation above the datum (cm), p is the pressure ($dynes/cm^2$), p_0 is the atmospheric pressure ($dynes/cm^2$), and ρ is the density of the fluid (g/cm^3). If p_0 is taken to be zero and we recall that $p = \rho g H$, we obtain

$$\Phi = g(z + H).$$

With the hydraulic or total head φ defined as Φ/g, we note that

$$\varphi = z + H$$

where z is the elevation head and H is the pressure head (substituting the moisture tension head ψ for unsaturated conditions).

MATRIC POTENTIAL

The complex air-water interfaces in an unsaturated medium are important in determining the pressure in the water. The forces acting in the air-water and solid-water interfaces are responsible for the so-called capillary phenomena and originate in the cohesive and adhesive forces between molecules. These forces attract and bind water in the soil and lower its potential energy below that of bulk water (Hillel, 1982).

The pressure potential in an unsaturated medium is usually called the capillary or matric potential. In 1907 Buckingham defined the capillary potential by assuming a conservative field of force, the gradient of which is the capillary potential (Novak, 1972). Gardner et al. (1922, in Richards, 1931) later noted that this potential was related to the pressure in the water films, and showed that porous clay apparatus could be used for its measurement. Richards (1931) describes experiments which show that the pressure in the liquid films is less than atmospheric and is a function of the quantity of liquid present in the medium. He stated that "(t)he forces acting in the boundary surfaces of liquids are directly responsible for all capillary phenomena and have their origin in the cohesive and adhesive attractions which are exerted between molecules."

CAPILLARY PRESSURE

As previously stated, when two immiscible fluids are in intimate contact, an interface is developed across which there is a discontinuity in pressure. There is a tendency for this interface to assume a configuration which minimizes the area of contact between the fluids. This is due to the free energy possessed by the molecules of the liquid lying on the interface (Richards, 1931). This is what causes the curved nature of the interface, as a sphere has the smallest proportion of molecules at the surface (Petrucci, 1985).

In a vertical capillary standing in water, a curved surface or meniscus is formed, and capillary rise takes place until the hydrostatic pressure balances the pressure difference due to curvature. Across the curved interface the pressure difference at any given point is described by

$$p_c = \Delta p = p_2 - p_1 = \gamma\left(\frac{1}{r'} + \frac{1}{r''}\right)$$

where p_1 and p_2 are the pressures in the fluids taken as the interface is approached from

their respective sides, γ is the surface tension, and r' and r'' are the radii of curvature of

the interface at the point (Carman, 1941). The magnitude of the pressure difference

depends, therefore, on the curvature of the interface which is a function of saturation. This

is known as the Laplace formula for capillary pressure, p_c (Bear, 1979). When the two

fluids being considered are air and water, the air is often considered to be at atmospheric

pressure ($p_2 = 0$) which defines the capillary pressure as a negative value, leading to the

use of the terms "suction" and "tension" in much of the literature, primarily that of soil

scientists. A related term is pF which is the logarithm to the base 10 of the matric suction

in centimeters of water (Stakman, 1966).

Pressure head is defined as the pressure divided by the specific weight of the fluid,

which allows the use of units of length, greatly simplifying calculations (Potter and

Wiggert, 1991). The matric suction in a sample can be measured with a tensiometer, and is

often referred to as capillary pressure head h_c, defined by Bear (1979) as

$$h_c = p_c / \rho g = -p_w / \rho g; \quad p_{air} = 0.$$

Fluid Movement

Fluid flow in porous media can occur in either a steady state or transient flow

condition. Flux, gradient and water content remain constant with time in a steady state

flow system, while they can vary in a transient flow system. Steady flow measurements are

generally less difficult to obtain and more accurate than transient flow (Hillel, 1982).

CONSERVATION LAWS

The flow of fluid is a mechanical process which must obey the laws of physics. The Navier-Stokes equation for the motion of a fluid, which relates the viscous, inertial, body and pressure forces involved in the flow, can be written

$$\frac{dv}{dt} = F - \frac{\Delta p}{\rho} + \left(\frac{\mu}{\rho}\right)\left(\frac{1}{3}\nabla\nabla \cdot v + \nabla \cdot \nabla v\right)$$

where ρ is the fluid density, v is the linear velocity, F denotes the body forces, ie. acceleration due to gravity, P is the pressure in the fluid, and μ is the viscosity. The solution of this equation is difficult even in free space where the boundary conditions may be known and easily stated. Use of this equation in heterogeneous, unsaturated media is limited due to the difficulty in describing the boundary conditions. Therefore, an alternate expression must be used to describe the motion of a fluid in such cases (Klute, 1952).

The flow of a fluid must obey the principle of conservation of mass. This is usually expressed for free space as: "the net excess of mass flux per unit time into or out of any infinitesimal volume element in the fluid is equal to the time rate of change of the fluid density in the volume element multiplied by the free volume of the element". This is stated mathematically as

$$\frac{\partial \rho}{\partial t} = -\nabla \cdot V$$

where ρ is the fluid density and V is the mass of fluid flowing through unit cross section in unit time. This must be modified for porous media where the entire pore volume is not available for fluid flow. For unsaturated media we may write

$$\frac{\partial}{\partial t}(\rho_b \theta) = -\nabla \cdot V$$

where ρ_b is the bulk density and θ is the moisture content on a mass basis. Replacing the

mass flux V ($=q\rho$) with the volume flux q (as defined below by Darcy's law) yields

$$\frac{\partial}{\partial t}(\rho_b \theta) = \nabla \cdot (\rho K \nabla \Phi)$$

where ρ is the fluid density. This is the general equation of unsaturated flow (Klute, 1952).

EQUATIONS OF FLOW

H. Darcy was the first to model the movement of water through porous media in

1856. In studying the flow of water through an early sand filter for the town of Dijon,

France, he came up with the empirical equation

$$Q = qA = -KA\left(\frac{\Delta p}{L}\right)$$

to predict the volumetric flow rate through sand under saturated, isothermal, and steady

state conditions. This relationship indicates that the flow rate Q is proportional to the

change in pressure Δp over the distance L by the product of the hydraulic conductivity K

and the cross-sectional area of the column A (Novak, 1972). Darcy's law is analogous to

Fourier's law in the flow of heat, to Ohm's law in the flow of electricity, and to Fick's law

in diffusion (Klute, 1952).

Darcy's law was also found to hold true for unsaturated flow if the driving force is

changed from a pressure gradient (Δp) to a potential gradient ($\Delta \Phi$). Darcy's law is valid

for unsaturated media at a given moisture content because in the unsaturated medium there are pores which are wholly or partly filled with air. Since air inclusions effectively prevent liquid flow through themselves, they could theoretically be replaced by a solid phase and the result would be a saturated medium (Richards, 1931; Corey, 1986). It is assumed that the compressibility of air is negligible in this analogy.

It may be seen then that the presence of air in the pores has the effect of reducing the volume of medium available for flow of the fluid and does not of itself invalidate Darcy's law. Due to the fact that the effective cross-section available for flow of the fluid is reduced in an unsaturated medium as compared to that of a saturated medium, the conductivity of an unsaturated medium is a function of moisture content, $K(\theta)$, and will decrease with decreasing moisture content of the medium (Klute, 1952).

Some limitations do exist for the application of Darcy's Law in porous media. Cases in which the flow rate is high enough to cause non-laminar flow, such as some limestones or cracked rock, preclude the use of the law. Reynolds number R_e, based on average grain diameter of the media, must be less than 10 when defined as

$$R_e = \frac{\rho v_d d}{\mu}$$

where ρ and μ are the density and viscosity of the fluid, d is the grain diameter and v_d is specific discharge, defined as volumetric flow rate over area (Freeze and Cherry, 1979).

Darcy's law for flow in the x-direction of an x, y, z coordinate system can be written as

$$q_x = -K(x, y, z, \psi) \frac{\partial \varphi}{\partial x}.$$

Flow in the other two coordinate directions can be described with similar expressions

(Freeze, 1969). In this case the hydraulic conductivity is expressed as a function of

position and matric suction head.

The equation of continuity for unsteady flow of a compressible fluid, is

$$-\left[\frac{\partial(\rho v_x)}{\partial x}+\frac{\partial(\rho v_y)}{\partial y}+\frac{\partial(\rho v_z)}{\partial z}\right] = \frac{\partial}{\partial t}(\rho\theta).$$

Substituting the appropriate form of Darcy's law into this equation and expanding the

right-hand term, the continuity equation becomes

$$\frac{\partial}{\partial x}\left[\rho K(x,y,z,\psi)\frac{\partial\varphi}{\partial x}\right]+\frac{\partial}{\partial y}\left[\rho K(x,y,z,\psi)\frac{\partial\varphi}{\partial y}\right]+\frac{\partial}{\partial z}\left[\rho K(x,y,z,\psi)\frac{\partial\varphi}{\partial z}\right] = \rho\frac{\partial\theta}{\partial t} + \theta\frac{\partial\rho}{\partial t}.$$

From this generalized equation of flow it is possible to develop the one-, two-, or three-

dimensional forms of the steady or unsteady flow equations for saturated or unsaturated

flow of a compressible or incompressible fluid through non-homogeneous, porous media.

The terms on the right-hand side of this equation represent the de-watering of an

elemental cube within the media, both from changes in the moisture content θ, and from

changes in the fluid density ρ. Any variation in hydraulic conductivity K with position in

saturated flow results from the inhomogeneity of the porous medium, while in unsaturated

flow, K varies with position even in homogeneous soils, due to the functional relationship

between K and moisture content (Freeze, 1969).

The flow equation for water in unsaturated soils was first formulated in 1931 by

Richards who approached the problem of capillary flow measurement using methods

which were theoretically and experimentally analogous to those used in the study of
conduction of heat and electricity.

Water is usually assumed to be incompressible for unsaturated unsteady flow, that
is ρ is constant and $\partial\rho/\partial t = 0$. For a homogeneous soil, $K(x,y,z,\psi)$ becomes $K(\psi)$ and the
one-dimensional, vertical form reduces to Richards' equation

$$\frac{\partial}{\partial z}\left[K(\psi)\left(\frac{\partial\varphi}{\partial z}\right)\right] = \frac{\partial\theta}{\partial t}.$$

The ψ-based form of this equation for one-dimensional, vertical, unsaturated, unsteady
flow becomes (Freeze, 1969)

$$\frac{\partial}{\partial z}\left[K(\psi)\left(\frac{\partial\psi}{\partial z}+1\right)\right] = C(\psi)\frac{\partial\psi}{\partial t}$$

if we recall that $\varphi = z + \psi$ and with the specific moisture capacity C defined as

$$C(\psi) = \frac{d\theta}{d\psi}.$$

The corresponding θ-based equation was derived by Philip (1957) using the concept of
diffusivity D where

$$D = K\frac{\partial\psi}{\partial\theta}.$$

The derived equation is

$$\frac{\partial\theta}{\partial t} = \frac{\partial}{\partial z}\left(D\frac{\partial\theta}{\partial z}\right) + \frac{\partial K}{\partial z}$$

where ψ and K are single-valued functions of θ (ie. hysteresis is ignored), and z is the vertical dimension, positive upwards. The corresponding one-dimensional horizontal form is

$$\frac{\partial \theta}{\partial t} = \frac{\partial}{\partial x}\left(D\frac{\partial \theta}{\partial x}\right)$$

where x is the horizontal space coordinate (Philip, 1991).

Poiseuille's Law applies to capillary flow from a tension-free source, and is stated

$$Q = \frac{\pi r^4 p}{8L\mu}$$

where Q is the volumetric flow rate, r is the tube radius, p is the pressure difference driving flow, L is the tube length and μ is the fluid viscosity. The flow into capillary tubes can be modeled using the force pulling the fluid ($2\pi r\,\gamma\cos\alpha$) acting on the cross-sectional area (πr^2). The equation then becomes

$$Q = \frac{\pi r^3 \gamma \cos\alpha}{4L\mu}$$

and can easily be solved for capillaries of various radii (Swartzendruber et al., 1954). This law also fails when high pressure gradients exist in the system (Richards, 1931).

Saturated Flow

Hydraulic conductivity is defined from Darcy's law as the proportionality constant K which contains media and fluid components as

$$K = \frac{k\rho g}{\mu} \ .$$

Traditionally, determination of K involves applying Darcy's law to results of laboratory testing. Saturated conductivity is also somewhat affected by temperature as μ is inversely temperature-dependent (Swartzendruber, 1969).

Malik et al. (1984) estimated the hydraulic conductivity from capillary rise experiments. The primary advantage cited by these authors was the great reduction in time necessary to obtain conductivity data as compared to standard methods which require complete saturation of the sample before testing. They referred to their method as the "Quick Capillary Rise" or QCR method. The validity of this approach was verified a few years later (Kumar and Malik, 1990) who found that the values obtained using QCR matched those determined by traditional methods.

Unsaturated Flow

When the effective pore space of a porous medium is no longer completely filled with a given liquid, the medium is said to be unsaturated with respect to that liquid. The type of unsaturated system, however, depends upon the nature of the second fluid occupying the vacated pore space. If the second fluid is another liquid, heterogeneous saturation results if the two liquids are immiscible. If the second fluid is a gas, or a mixture of gases such as air, then the resulting three-phase system describes what is commonly considered unsaturated flow. The process of water flow in such an unsaturated system could also be described as a two-fluid problem in immiscible displacement, where water and air are the fluids (Swartzendruber, 1969).

Unsaturated media exhibits adsorption in addition to capillary phenomena which causes the formation of hydration "envelopes" over the surface of the particles. Particularly under greater suction conditions, the primary water retention mechanism is adsorptive rather than capillary. In this case retention capacity depends more on media texture than structure (Hillel, 1982).

The movement of a fluid along a solid surface depends upon both adhesive and cohesive forces. The initial wetting of the solid by the liquid depends primarily upon adhesive forces. If the surface densities of free energy for the air-liquid, air-solid and liquid-solid interfaces for a given three-phase system are γ_1, γ_2 and γ_{12} respectively, it may be shown that

$$\gamma_1 + \gamma_2 - \gamma_{12} = W = \gamma_1(1 + \cos\alpha)$$

where W is the work necessary to separate a unit area of liquid from solid and α the contact angle between the liquid and the solid. If $W < 2\gamma_1$, α may vary anywhere between 0 and 180 degrees. If, however, $W \geq 2\gamma_1$ then α is zero and the liquid will spread over the surface of the solid and is said to wet the solid. Once the solid is wetted adhesive forces primarily hold the liquid film firmly in contact with the solid surface and are no longer effective in producing liquid motion. Additional liquid outside the adsorbed films is free to move as a result of unbalanced forces (Richards, 1931).

In a liquid-saturated porous media system the process of water transport is one of bulk flow. However, the existence of the gaseous phase in an unsaturated system allows also for the possibility of water transport in vapor form. It is generally felt that vapor-phase transport is relatively insignificant compared with the liquid-phase transport, unless

the soil water content is very low or when temperature variations or salts induce significant vapor-pressure gradients (Gardner, 1958; Swartzendruber, 1969).

Klute (1952) credits Childs and George with establishing the method of calculating the functional relationship $K(\theta)$ between conductivity and moisture content of an unsaturated system from the moisture characteristic curve. This curve is a plot of the matric potential versus the moisture content of the transport medium. They related the conductivity of an unsaturated medium to the geometry of the void space using a pore size distribution curve as a measure of the latter.

Some of the factors which can affect flow in unsaturated media are entrapped air which may go into or come out of solution, dispersion of aggregates in the fluid, bacterial growth and action during the flow period plus the variation due to moisture content (Klute, 1952). The temperature dependence of surface tension, which plays a role in the moisture state of unsaturated media, has some effect on the ψ-θ relationship and thereby also on conductivity (Swartzendruber, 1969).

Wind (1966) used evaporation from a saturated column to determine unsaturated hydraulic ("capillary") conductivity. The total weight of the column was determined daily along with changes in the moisture content and tension at various depths from the column surface. He found that measurement of $K(\psi)$ determined with the aid of Bouyoucos' electrical nylon units, are fairly accurate at moisture tensions between 0.1 and 20 atmospheres. Below 0.1 atmospheres they lack accuracy.

He calculated the velocity of flow at different depths from the changes in moisture content and weight. For every day, at every depth the velocity of flow is known; it equals

the amount of moisture lost by the soil below. The potential gradient belonging to this flow was calculated from the moisture tension readings, thereby allowing calculation of $K(\psi)$ with the formula

$$q = K(\psi)\left(\frac{d\psi}{dx} - 1\right)$$

where q is the velocity of flow in mm/day, and $d\psi/dx$ is the potential gradient in cm/cm.

It is known that the hydraulic conductivity becomes a function of matric potential (and thus water content) in unsaturated media. The relationship between ψ and θ is described functionally in the moisture characteristic (or moisture retention) curve. This curve is not single-valued, but rather dependent upon the moisture history of the sample, such as whether fluid is draining from or being added to the media. This multi-valued functionality is referred to as hysteresis, and affects interfacial tension and wettability depending upon whether the fluid-fluid interface is advancing or receding.

A higher saturation level can be obtained at a given value of tension for a sample being drained than for one during imbibition. Air can also be entrapped during imbibition, which will not permit the complete saturation of pore space. During the draining cycle, once the local pressure has increased to allow fluid movement through a constriction or neck, adjoining larger pores will desaturate almost immediately (Bear, 1979). Refilling the same pores requires less pressure as the pressure is dictated by the size of the pore, not the neck (Parlange, 1980). This phenomenon is often referred to as the "ink-bottle" effect.

Other authors have attempted to account for the hysteresis phenomenon in their modeling of unsaturated flow (Miller and Miller, 1955; Philip, 1964). As stated by Philip (1991), hysteresis does not invalidate the use of the equations of flow as long as the $\psi(\theta)$

function chosen is appropriate to the flow being studied; a wetting curve is appropriate for absorption or infiltration, while a drying curve is appropriate for water removal processes.

Upward Flow Through Porous Media

Evaporation

There is general agreement among scientists that the rate of evaporation from a soil is controlled by either the capacity of atmosphere to evaporate water or by the soil's capacity to transmit water to the surface. At relatively shallow depths the atmosphere is typically the limiting factor (Corey, 1986). Up to a limiting rate the steady upward flux from a water table will meet the potential rate dictated by the atmosphere. This rate is defined by the soil hydraulic conductivity properties and can be calculated using the Darcy-Buckingham equation for steady soil water flux. This requires knowledge of $K(\psi)$ which may not be known and can be difficult to obtain. Alexander (1982) examined a number of methods of predicting $K(\psi)$ for a variety of soils.

Anat et al. (1965) studied steady upward flow from water tables related to evaporation. They focused on soil parameters which determine the maximum rate of upward flow as well as the effect of the moisture history of the soil (rising vs. falling water table). They found that the flow rate following a drainage cycle can be 100 times greater than following imbibition into a dry soil. The parameters included in their estimation equation were pore-size distribution index, depth from surface and bubbling pressure.

Capillarity

A difference in pressure between two points in a liquid film, such as that found in unsaturated media, causes the liquid to move in the direction of lower pressure. The term capillarity was used by Richards (1931) to describe "liquid systems where the pressure distribution is determined by the surface tension and curvature of a gas-liquid interface."

Capillary rise can be defined as the movement of a liquid in an upward vertical direction due to molecular forces of attraction and adsorption. It can be clearly demonstrated by lowering a small-diameter tube into standing water and observing the level of the water in the tube. This level will be at some distance above the free water level of the water supply (for tube diameters smaller than a critical value).

This rise is a result of attraction between the tube and the molecules of water, and the surface tension characteristics of the water. The upper surface of the water assumes a curved shape and is referred to as the meniscus. This surface meets the tube surface at an angle called the contact angle. This angle is dependent upon the material of the wall, impurities on the wall surface and the surface tension of the liquid. The contact angle can approach 0° for chemically clean tubes, which allows for the maximum rise height distance.

In such an unsaturated three-phase system, the curved meniscus obeys the following equation of capillarity

$$p_0 - p_c = \Delta p = \gamma \left(\frac{1}{r_1} + \frac{1}{r_2} \right)$$

where p_0 is the atmospheric pressure, usually considered to be zero, p_c is the pressure of the water, γ is the fluid's surface tension, and r_1 and r_2 are the principal radii of curvature of a point on the meniscus (Hillel, 1982).

At equilibrium the vertical forces on the water column in a small-diameter tube must be equal. This can be described by the equation

$$h\pi r^2 \rho g = 2\pi r \gamma \cos\alpha$$

where h is the height of capillary rise, ρ is the density of the water, g is the force of gravity, γ is the surface tension of the fluid and α is the contact angle (Baver, 1956; Terzaghi and Peck, 1967). The left-hand term describes the downward force due to gravity acting on the volume of the water column, while the right-hand term indicates the upward force holding the column in the tube. The surface tension force acts on the tube wall along the surface of the meniscus formed at the fluid-fluid interface. This surface meets the tube at an angle equal to the contact angle, so the vertical component of this force is equal to $\gamma\cos\alpha$ which acts over the perimeter of the meniscus.

The theoretical maximum height of capillary rise for a liquid in a tube can be determined by solving for h in the above equation. The rise tends to occur as the liquid molecules are attracted to the solid surface and the contact angle α is close to zero. A column of liquid is then pulled upward by these adsorptive forces. The liquid will continue to rise into the tube until the downward forces on the liquid column equal the upward forces, with h increasing as $\cos\alpha$ decreases toward a value of zero.

In the case of capillary rise in a porous media such as soil or sand, the tube is replaced by an interconnected network of voids between the particles. This pore space is

almost impossible to completely describe in size and direction, although it acts similarly to a bundle of tubes in its ability to raise a liquid through capillarity. In this case the liquid is transported in a film which exists above a layer of liquid one or two molecules thick which is adsorbed to the solid surface of particles. This layer is sometimes called a hydration envelope (Hillel, 1982). The transport film becomes thicker in areas of contact between two particles where hydration envelopes intersect.

Carman (1941) declared the height of capillary rise to be an important indication of a media's relative capillary potential in comparing any two soils or sands. He showed that the maximum height of capillary rise could be estimated from the particle size and porosity of a fine sand, and determined that, although the force driving capillarity is much greater for a fine sand than for a coarse one, water enters the coarse sand at a faster rate. He provided theoretical calculations of upward capillary movement of water into initially dry sands. Wladitchensky (1966) suggested that the height of capillary rise is also dependent on the hydrophilic character of the pore walls.

Wadsworth and Smith (1926) studied the effect of the cross-sectional area of soil columns on capillary rise. Square cross-sectional columns used varied from 1 inch to 12 inches, and the media used was classified as Yolo fine sandy loam which passed through a 2 mm. mesh. They found that in general large columns show a greater rise after a given time than small columns. They found that the size of the container was of greatest importance in columns with a cross-sectional area of less than twenty-five square inches. They also found that a fairly uniform and consistent moisture content exists at all points in any horizontal plane within the column.

Some of the factors which have an effect on capillary rise include the initial moisture content and the degree of compactness of the media. Capillary rise height increases as initial moisture content increases (Ijjas, 1966; Wladitchensky, 1966). As the compactness of the media was increased, the maximum capillary rise height also was increased. Ijjas (1966) measured the discharge due to capillary action over an impermeable barrier. He found that at capillary rise heights greater than 6 cm this volumetric discharge was greater for a compact soil than for a loose soil. He surmised that this was due to the greater role of media permeability at shorter rise distances.

Early studies speculated that the rate of capillary rise in loam soil increased with temperature, with looseness of packing, and with original moisture content of soil. It was also observed that rise was more rapid in columns of sand particles of mixed sizes than for particles of uniform size. Ijjas (1966) found that the rate of capillary rise into an initially dry soil was greater for a less compacted soil, but only within the first 100 minutes.

Malik et al. (1989) used saturated hydraulic conductivity and wilting point to obtain soil constants which gave maximal capillary rise flux as a function of rise height z. In an earlier study Malik et al. (1984) used the rate of capillary rise in (dry) porous media columns during the first time segment ($t < 2$ hours) to validate Poiseuille's law by the straight line relationship between dz/dt and $1/z$. This allowed the quick estimation of pore geometrical properties (formation factor, shape factor and equivalent pore radius) and capillary constants for a flow system, including hydraulic conductivity.

A zone exists above the saturation or free water level in a soil which has been referred to as the capillary fringe, or tension-saturated zone. The pores in this zone are saturated, but the capillary pressure is less than atmospheric. This anomalous situation

exists due to the existence of the air entry or bubbling pressure in the moisture characteristic curve. The media will remain saturated until this pressure is reached, at which point the largest continuous pore will desaturate. This pressure corresponds to a height above the free water level, so below that height the media will remain saturated. The capillary fringe height of fine-grained media will extend higher than that of a coarse-grained media due to the greater negative value of bubbling pressure (Freeze and Cherry, 1979).

Capillary Siphoning

Capillary siphoning, or wicking, can be defined as the movement due to capillarity of a fluid over an impermeable barrier in unsaturated media. The siphoning phenomenon was described briefly by Terzaghi and Peck (1967), but without reference to other work in the area. That text states that capillary siphoning was the cause of losses from twelve miles of canals in Germany in the range of 450 gal/min at a rise distance of 12 inches. This was reduced to 100 gal/min when the rise distance was increased to 16 inches.

Studies were done in Hungary on the losses from canals due to seepage over impermeable barriers, but only some of this work has been translated into English (Ijjas, 1966). It has been possible, however, to glean some information from the data reported in Ijjas' Hungarian-language paper (Ijjas, 1965).

In his papers Ijjas looked at the seepage over an impermeable barrier in a canal wall for both a medium (A; $D_{10} \cong 0.13$ mm, $U = 2.3$) and a fine (B; $D_{10} \cong 0.08$ mm, $U = 2.7$) sand. He confirmed the generally accepted fact that the height of capillary rise

increased with initial moisture content θ_0, and determined that the ultimate rise height was greater with decreased media porosity ϕ. However, during the initial period of wetting (<100 minutes) the rate of capillary rise was greater in a more porous media.

He also examined the "(e)ffect of the vertical distance (z) between the upper edge of the sealing and the canal watersurface on the magnitude of capillary losses" (Ijjas, 1965). Ijjas' work found that system outflow Q decreased logarithmically as z was increased. He measured values of Q ranging from 4.5 L/sec km (27.8 gpd/ft) at $z = 2$ cm to 1 L/sec km (6.9 gpd/ft) at $z = 10$ cm. While he did not state specifically, it is believed that these results were from the medium sand (A) media.

Ijjas further examined the dependence of the capillary outflow upon the vertical distance H_w between the free-water surface elevations upstream and downstream of the barrier. He found that Q increased by 20% at $z = 2$ cm and 50% at $z = 10$ cm when H_w was increased from 65 cm to 115 cm. The outflow increased with H_w (at a given value of z), more dramatically at smaller values of z, with the greatest rate of increase for H_w less than 65 cm. For example, when $z = 5.0$ cm Q increased from 1 L/sec km (6.9 gpd/ft) at H_w = 10 cm to 2.5 L/sec km (17.4 gpd/ft) at $H_w = 50$ cm.

He found that for $z > 6$ cm the outflow was greater from media with less pore volume ($\phi = 37.6\%$), while at $z < 6$ cm the outflow was greater for media with more pore volume ($\phi = 43.0\%$). He attributed this to the effects of media permeability on unsaturated conductivity.

The effect of the thickness of media (v_m) protecting (perpendicular to) the impermeable barrier on the outflow from the system was also examined by Ijjas. His study

found that maximum outflow occurred at greater values of v_m as z increased. The greatest amount of seepage was measured when v_m was about 13 cm for $z = 5$ cm, while at $z = 0$ cm it was recorded when $v_m = 9$ cm ($H_w = 20$ cm). Maximum seepage for $0 < z < 5$ cm occurred at approximately $v_m = 15$ cm.

Ijjas found that the finer media (B) allowed higher outflow at values of z greater than about 2.5 cm (at $v_m = 15$ cm and $H_w = 20$ cm). This media also had a higher uniformity coefficient value indicating a wider distribution of particle sizes. The influence of media distribution on outflow results was not described, and is part of the current study.

Application to Wastewater Treatment

The capillary mechanisms researched and discussed in this thesis are being investigated in order to understand the hydraulic capacity of the aerobic capillary zone of an upflow wastewater treatment system. This system has been introduced as an option for secondary treatment in small-scale onsite wastewater systems. This section will provide an overview of the utility of capillary siphoning in this zone of wastewater treatment.

The treatment of wastewater before final disposal or reuse is concerned with the reduction of various constituents which can cause environmental and/or health concerns. Examples of these are nutrients such as nitrogen and phosphorus, harmful micro-organisms, and organic solids. Each of these can be treated by one or more of the following pathways: physical or mechanical isolation, chemical conversion, and biological decomposition or transformation.

Filtration can provide a physical means of removing solids from wastewater being treated. Primary treatment, such as that found in a septic tank, can remove the bulk of the gross solids from wastewater through segregation of settleable and floatable portions. Therefore secondary treatment should provide a means of removing suspended solids. In capillary rise mechanisms segregation of particles can occur through physical filtration as the fluid moves through the media matrix. Larger particles in suspension may also be separated during the upward vertical film flow as gravitational forces will likely be stronger than the forces suspending the particles in solution.

Another benefit to the capillary siphoning mechanism in a system is that aerobic treatment is accomplished without significant loss in elevation. This may be particularly important in system configurations where the final disposal site can then be reached without the addition of an external energy input such as a pump.

The nutrients in wastewater promote biological activity—possibly the primary cause of clogging which reduces the infiltrative ability of soil adsorption fields (Otis, 1985). Nutrient reduction is also imperative to avoid groundwater pollution, for example the nitrate (NO_3) form of nitrogen which can be harmful to children and during pregnancy. Therefore, the reduction of nutrients, particularly total nitrogen, is a major focus of onsite wastewater treatment. Nitrogen can exist in wastewater as organic N, as ammonium ($NH_4^+ - N$), and in the oxidized forms of nitrate ($NO_3^- - N$) and nitrite ($NO_2^- - N$) (USEPA, 1980).

Denitrification can be an efficient method of reducing total nitrogen, but this process requires oxidized forms of nitrogen such as NO_3 or NO_2 which then follow the denitrification pathway

$$NO_3 \Rightarrow NO_2 \Rightarrow NO \Rightarrow N_2O \Rightarrow N_2 .$$

NH_4^+-N must be converted to NO_3^- by the aerobic process of nitrification before

denitrification can take place (Eastburn and Ritter, 1985). The unsaturated conditions

which must exist in the region of capillary siphoning provide the oxygen required for this

conversion.

After wastewater has been exposed to the anaerobic conditions which typically

exist in a septic tank, 65 to 75% of the nitrogen has been decomposed by micro-organisms

from the organic form to ammonium (USEPA, 1980). In a subsequent aerobic

environment this ammonium can then be oxidized by select bacteria to nitrite and

ultimately to nitrate forms which are necessary for denitrification. This nitrification is a

biological reaction which consists of at least two steps: nitrobacter produce nitrite from

ammonium, and nitrosomonas (primary among other micro-organisms) convert nitrite to

nitrate (Laak, 1982). Aerobic biological treatment processes can also significantly reduce

pathogenic organisms in the wastewater (USEPA, 1980).

Chapter 3

EXPERIMENTAL PROCEDURES

Transport Media

The media used in these studies was obtained from locally operating commercial

suppliers of sand and gravel. This material was selected from within the grade of sand

typically used in transportation and other construction; the State of Michigan's

Department of Transportation (MichDOT) uses the general media designation of "2NS"

for sand in this range. The specifications for MichDOT's 2NS grain size distribution range

can be found in Table 1.

Table 1. MichDOT Grading Specifications for 2NS Sand.

Sieve Mesh Opening, mm	Total Percent Passing*
9.5	100
4.75	95-100
2.36	65-95
1.18	35-75
0.60	20-55
0.30	10-30
0.15	0-10

* Based on dry weight.

Media Preparation

No special preparation of the media was done beyond air-drying. For this the sand

was spread out to a depth of no more than one centimeter on absorbent paper and allowed

to dry for at least a week. The air-dry sand was then separated into a number of classes

according to the particle diameter. This was accomplished through the use of an electric

RO-TAP Testing Sieve Shaker[1] and a nest of sieves of varying sizes. Batches of

approximately 300 grams of the sand were poured into the top sieve of the nest, which

varied from the largest sieve opening at the top to the smallest sieve opening at the

bottom. The sieve shaker was then switched on, providing circular lateral motion to the

nest while simultaneously tapping the nest's cover plate with a regular hammering action

to provide vibration. Each batch was allowed to run under these conditions for 3 minutes.

The nest was then disassembled and the sand in each sieve collected and weighed

in order to determine the actual grain size distribution of the original 2NS media. The

particles in each separate size class should then have been no larger than the opening of

the sieve above it, and no smaller than the size of the sieve upon which it was captured.

The distribution of particle sizes used for each of the treatments can be seen in Table 2.

The media separates were then mixed together in predetermined amounts in order to

achieve the prescribed grain size distributions for the comparative portion of this work.

The proper amount of each separate was added to a five gallon plastic container which

was rotated at a 45-degree angle while the sand was thoroughly mixed by hand.

---

[1] W.S. Tyler Co., Cleveland, Ohio USA

Table 2. Grain size distributions for all treatments by percent passing through sieve.

Mesh Opening, mm	D_{10} = 0.1 mm U = 2.5	D_{10} = 0.2 mm U = 1.5	D_{10} = 0.2 mm U = 2.5	D_{10} = 0.2 mm U = 4.5	D_{10} = 0.4 mm U = 2.5
6.350				100.0	100.0
4.760				98.5	99.5
3.360			100.0	95.0	98.0
2.000			99.5	85.0	91.0
1.651			99.0	80.0	86.0
1.410			98.0	75.0	79.0
1.190	100.0		95.5	70.0	70.0
0.850	99.0	100.0	87.5	57.0	50.0
0.600	96.0	98.0	70.0	43.0	28.0
0.300	72.0	60.0	30.0	20.0	3.0
0.212	50.0	15.0	13.0	11.0	0.0
0.106	12.0	0.0	0.0	3.0	
0.056	0.0			0.0	

Geometric Description

The basis of the experimentation explained herein is the comparison of the capillary hydraulic transport capabilities of various grain size distributions of unconsolidated sand media. In order to characterize the geometry of the media used in the study, two standard engineering descriptors were selected: the effective size and the uniformity coefficient.

The effective size D_{10} describes the sieve opening through which only ten percent of the media will pass (on a mass basis). When this number is divided into the D_{60}, or the sieve opening through which sixty percent of the media will pass, the resultant is referred to as the coefficient of uniformity U. A smaller value for U indicates that the media is considered to be fairly uniform, with most of the particles' diameters falling within a small range; conversely, media with a wide range of particle sizes would have a larger coefficient of uniformity.

Capillary Siphon

Design

Inverted U-shaped containers were designed to hold the various media distributions in a configuration which would allow the simulation of fluid transport over an impermeable barrier. This shape consisted of three continuous sections: an upflow leg which would be immersed in the water reservoir tub, a horizontal section which supports the container, and a downflow leg which hangs freely allowing the water which is moving through the siphon to drip out for collection and measurement. These containers were referred to as 'siphons' due to their effective movement of water over the rim and out of the reservoir tub.

Construction

The siphons were constructed from commercially available rigid plastic 'tubes' which had a square cross-section and were manufactured for use as roof eavestrough downspouts[2]. The inside of the siphon was approximately 6.2 cm across, with rounded corners and a wall thickness of one to two millimeters. Tightly sweeping 90-degree ells were used to connect the straight tubes and create the U-shape of the siphon.

All siphon parts were cut to the same dimensions and the siphons were constructed to the same specifications to ensure physical similarity. A vertical cross-section of a typical finished siphon can be seen in Figure 1. After the parts were cut, the edges were filed and cleaned to remove any plastic burrs. The siphons were then assembled, with the pieces

---

[2] Rain-Go Downspout, Genova Manufacturing Co.
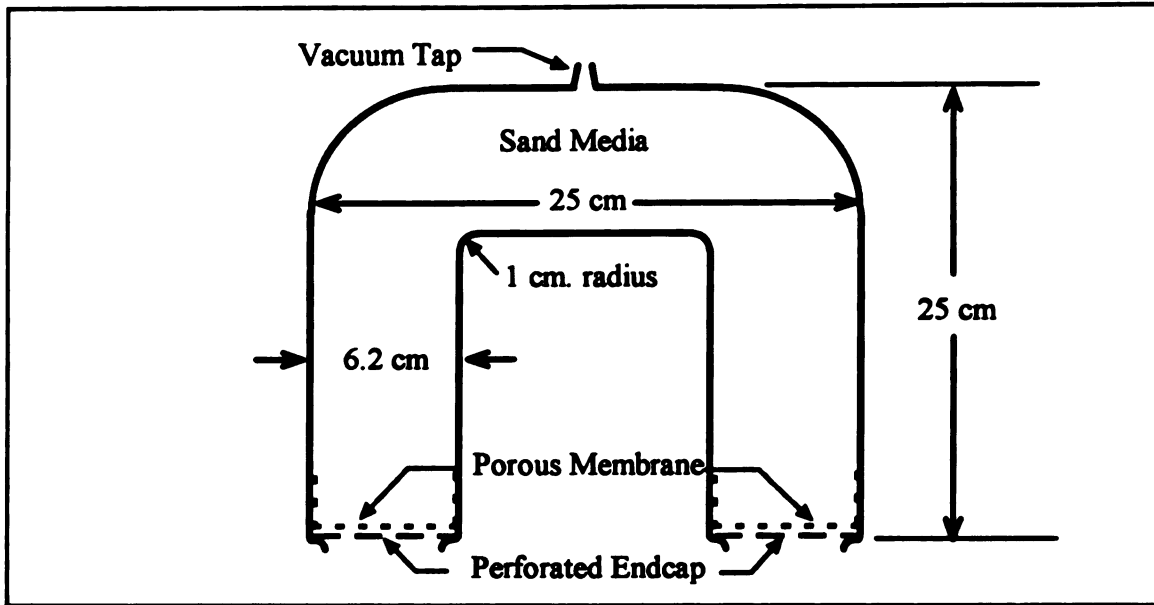
Figure 1. Cross-section of a sand-filled capillary siphon.

bonded together with PVC cement and all joints sealed with silicone caulking compound for watertight construction. Each siphon was later filled with water in order to test for leaks. The siphons were filled with the appropriate media as described under Sample Preparation later in this chapter.

Once the siphon had been filled with media the ends were capped. The caps consisted of tubing accessory pieces which fit tightly over the straight 'legs' of the siphon, and then reduced to a size which could fit inside the straight tubes. This reduction allowed for the placement of a rigid plastic end-plate which provided structural containment of the siphon media. These plates were adequately perforated to allow free movement of water into and out of the siphon. The granular media was actually contained within the siphon by a fibrous geo-membrane typically used as a porous wrap around agricultural drainage tile.

This was placed between the media and the perforated end-plate before the endcap assembly was caulked in place. Once this construction was completed, the siphons could be inverted so the legs were oriented downward for final placement on the support structure. At this point taps were installed at the midpoint of the top of the horizontal section for vacuum saturation and to provide atmospheric pressure within the siphon container.

Laboratory Setup

Experimentation for this study was conducted in the Soil and Water Laboratory of the Department of Agricultural Engineering in A. W. Farrall Hall on the campus of Michigan State University in East Lansing, Michigan USA. Tests were run between late March and mid-June 1996 with measured ambient temperatures ranging from 23.5° C to 25.0° C and relative humidity between 15% to 77%.
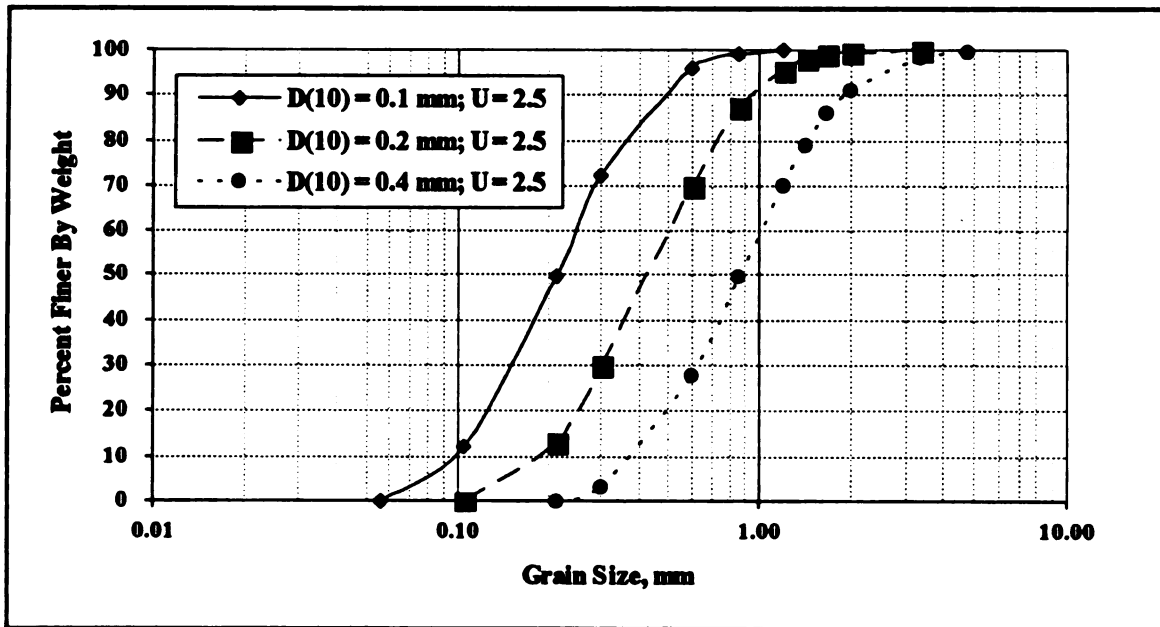
Figure 2. Grain-size distributions for experimental media of various effective sizes.

Experimental Design

The distribution treatments chosen for comparison consisted of three different effective sizes, all with similar uniformity (D_{10} = 0.1, 0.2 and 0.4 mm; U = 2.5), and three different uniformities, all with similar effective sizes (U = 1.5, 2.5 and 4.5; D_{10} = 0.2 mm). Grain-size distributions for these media can be seen in Figures 2 and 3, respectively. Three replicated samples of each treatment were established for statistical purposes. This results in a total of fifteen different siphons which were built and filled with the appropriate media distributions (the distribution with D_{10} = 0.2 mm and U = 2.5 being common to both comparisons). The siphons were coded according to the distribution parameters with the first two numbers signifying the effective size, the second two numbers signifying the uniformity, and the fifth character signifying the replicate sample code (decimal points were dropped). For example, the siphon code "0145A" signifies an effective size of 0.1 mm, a uniformity coefficient of 4.5, with the sample being in the first ('A') set of replicate units.

Support Structure

A structure was designed and built which served to provide support for the siphons as they were used in this study. The structure consisted of three identical wooden racks upon which the siphons were placed and separated into the three replicate groups (A, B and C). The racks were constructed so that the upflow legs of each siphon hung down into a plastic reservoir tub so that almost the entire upflow leg could be kept in a saturated state. The siphons would then remain stationary throughout the experimentation as the
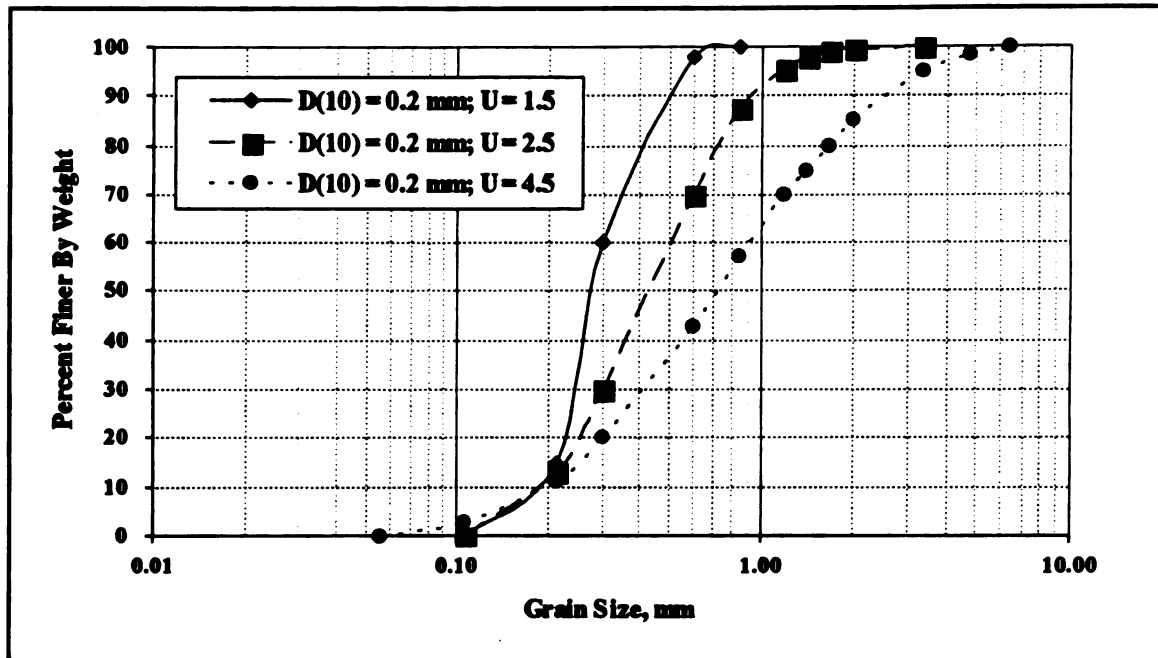
Figure 3. Grain-size distributions for experimental media of various uniformities.

level of the water in the tubs was lowered incrementally, and system outflow readings

obtained.

The structure kept the outflow leg of the siphons about 10 cm above the benchtop

so that either the water disposal tub or a flow sample collection container could be placed

under the outflow leg when needed. The reservoir tubs, on the other hand, were elevated

by the structure so that the upflow legs were about 1 cm above the bottom of the tub. This

made possible a range of capillary rise distances of 1 to 12 cm.

Water Supply System

Water was supplied to the reservoir tubs and kept at constant elevations in all three

tubs through the use of supply bottles combined with a constant head chamber system (ie.

Marriotte bottle). The constant head chamber (CHC) was a glass cylinder with an inside

diameter of about 5 cm which was supported vertically above the benchtop. The bottom of the chamber tapered to a connection with Tygon tubing which was manifolded to the three reservoir tubs. The top of the chamber was plugged with a rubber stopper containing three holes. One hole held a rigid plastic tube which extended from about 5 cm above the stopper to about 5 cm above the bottom of the chamber; the bottom of this tube provided the elevation of atmospheric pressure which defined the constant elevation of water in the reservoir tubs. The second hole contained tubing which also extended to about 5 cm from the bottom of the chamber and provided water to the chamber from the supply bottles. The third hole also contained tubing which only extended to the bottom of the rubber stopper; this tube connected the air space in the chamber with the air space in the two supply bottles.

The two 20-liter glass supply bottles were connected to the constant head chamber so that separate, continuous air and water lines existed between all three pieces of the system. This allowed the CHC to supply water on demand to the reservoir tubs as the siphons moved water out of the tubs. This mechanism worked as follows: as water was siphoned out of the tubs the water level in the tubs was lowered; this caused the water level in the CHC to also decrease creating a vacuum in the air space of the supply system. As this vacuum increased in the chamber's air space, air was drawn through the atmospheric pressure tube and bubbled up into the air space of the chamber. This temporarily equalized the pressure in the constant head system. Figure 4 shows a schematic diagram of the constant head supply system.

The continuous air and water lines between the CHC and the supply bottles
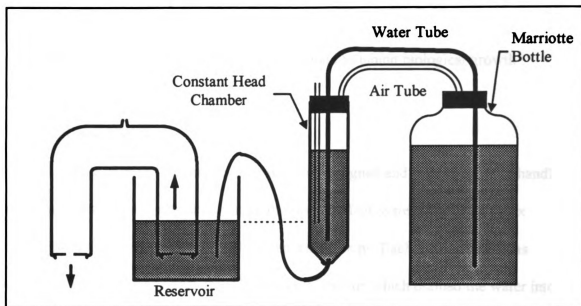
Figure 4. Schematic diagram of constant level water supply system.

increased the amount of time before the system needed to be refilled. This had to be done

before the CHC water level lowered to a critical elevation—the bottom of the atmospheric

pressure tube—when air could enter the water line, thereby destroying the integrity and

utility of the constant head device.

For the primary experimentation of this study distilled water was used exclusively

in the supply system in order to eliminate unwanted variables possibly associated with

minerals contained in municipal water supplies. This supply water was also disinfected on

a weekly basis with the addition of 5.25% Sodium Hypochlorite (NaOCl) solution[3]. This

reduced the possibility of biological growth both within the siphon media and throughout

---

[3] Household Bleach, Clorox Corporation

the supply system. The NaOCl solution was added to achieve a concentration of 10 ppm Cl_2 in the supply water which was deemed adequate to inhibit biological growth[4].

Water Disposal System

A collection and disposal system was also designed and built in order to handle the water which had already passed through the siphons. This system consisted of six collection tubs: two for each of the three replicate groups. Each of these tubs was equipped with a drainage port near the bottom of the tub which drained the water into flexible tubing which was then manifolded so that all of the tubs' water eventually ran through a single hose which emptied into a floor drain. The design of this system allowed for continuous, unattended disposal of the water as it moved through the siphons. The drainage ports were constructed from quick-release tubing connectors which allowed the tubs to be easily removed so that the flow volume measurement containers could be placed under the siphons for data collection.

Sample Preparation

In order to obtain useful comparative data across the various treatments, all siphons were subjected to the same preparation before data collection was begun. A protocol was followed which could be reproduced by others attempting to confirm, or build upon, the data described in this work. The three replicates within each treatment were prepared simultaneously and identically.

---

[4] Correspondence with Dr. Blaine Severin, Michigan Biological Institute, East Lansing, MI USA

Care was taken when packing the siphons with the granular media as it was important to achieve similar bulk densities between siphons, and cross-sectional uniformity throughout the length of each siphon. Similar bulk density was desired to reduce the chance of porosity differences between replicated samples of any given treatment, and to eliminate density as a variable between treatments. Since each siphon was physically similar, resulting in the same volume ($1370 \, cm^3$) for all siphons, the same mass of dry sand ($2200 \, g$) was packed into each unit. This results in a bulk density of $1.6 \, g/cm^3$ which corresponds to a porosity of 0.38, described by Corey (1986) as normal for unconsolidated sand media. Uniform cross-sectional makeup was achieved by filling each siphon from both of the open ends alternately using a 30 cm long pipe with 4 cm inside diameter. This pipe was placed into the open end of the siphon and filled with media through a funnel. As the pipe was slowly removed, the sand filled the siphon and was settled by light tapping on the outside of the siphon with a hammer. This procedure was continued until the prescribed mass of sand had been packed into the siphon container.

Vacuum Saturation

The siphons were all vacuum saturated so that a definite starting point could be defined before data collection was started. This is very important given the effect that the moisture content of the transport media has been shown to have on capillary rise phenomena. Vacuum saturation was utilized in order to best evacuate air from within the media matrix.

All three replicates within a treatment were placed in a water-filled tub so that both the upflow and the downflow ends were submerged, but the vacuum taps kept above the water surface. The replicates were then all connected to a single vacuum pump using a manifolded tubing system. This tubing was connected to a 500 ml laboratory vacuum flask which acted as a water trap to keep moisture out of the vacuum pump. The pump was run at a vacuum pressure of 25 mm of Hg until virtually no air was observed moving out of the siphons through the transparent vacuum taps.

System Equilibration

The vacuum hoses were then removed and the siphons were placed on the support structure with only the upflow leg immersed in water contained by the reservoir tubs. Air which may have been trapped in the submerged upflow endcap was completely evacuated to eliminate the chance of air movement into the siphon media in the saturated portion of the upflow leg. The downflow leg of the siphons were allowed to drain freely (into the disposal tubs) which initiated the siphoning mechanism within each unit.

The CHC height was initially set so that the water in the reservoir tubs was maintained at a level which corresponded to an capillary rise distance of 2.0 cm. Once all of the siphons were properly prepared and set on the support structure, they were allowed to equilibrate at this initial rise distance for 11 days before data collection commenced. This idle time was found to be necessary in order to allow the water movement through the system to reach a point of constant outflow.

Data Collection

The purpose of the primary data collection in this study was to quantify how the transport media chosen for transmission of water over an impermeable barrier affects the rate of water movement through the system by capillary phenomena at various rise distances. Therefore, the primary data measurement parameter was the amount of water which collected over a set period of time for each treatment at each capillary rise distance. In some instances this volume of water was relatively small, leading to possible errors in measurement. The mass of water was determined to be a more accurate account than the volume due to more accurate instrumentation.

Collection of data was begun once a constant volumetric outflow rate from the system was achieved. The data were collected from all siphons within a treatment set simultaneously, and from all treatments sequentially. Containers were placed under the downflow leg of each siphon and the time noted. The tare weight of each container was previously recorded and the containers numbered. When the collection containers were close to being filled, they were removed and weighed on a laboratory balance. This time varied from 10 to 55 minutes depending upon the flow rate of the system. The gross weights were recorded and the process repeated twice more for a total of three consecutive readings for each of three replicate samples of each treatment.

The only adjustment which was made in the system configuration between sets of readings was a successive, step decrease in the water level in the reservoir tubs (which corresponds with an increase in the capillary rise distance). After each set of readings were taken at a given rise distance, the CHC was lowered by 1 cm which allowed the level in the reservoirs to lower as water moved through the siphons. An equilibration period of at

least five days was allowed once the CHC was adjusted to a new level (as determined from preliminary experimentation described below).

Collection Containers

Collection containers were carefully designed and built in order to minimize the possibility of evaporation of the water during the collection period. The end of the siphons' downflow legs were tapered to allow a tight fit with the collection container. The body of the container was constructed from sections of the same material as the siphon body. At the beginning of a collection period the rim of the container was slipped up over the end of the taper and a block inserted under the container to hold it snug against the siphon's endcap while still providing adequate ventilation. The containers had a maximum capacity of 350 ml of water.

Determination of Capillary Flux

A spreadsheet was created which converted the raw collected data into a measure of the capillary flux through the siphons. The flux in this case is defined as the volume of water which passes through a unit cross-section of upflow media area per unit time (dimensions: $[L^3/\{L^2 * T\}] = [L/T]$). The input to the spreadsheet consisted of the beginning and end times of the run, the final weight of each container holding the individual flow volumes, and the container number. From this information the flow rate was calculated, then divided by the cross-sectional area of the capillary upflow zone, with the resultant being the capillary flux which was reported in units of centimeters per hour. Copies of these spreadsheets can be found in the Appendices.

Related Experimentation

Time to Equilibrium

A steady state was required by the active capillary siphons before flow measurements were taken in order to accurately compare the capillary flux through the various treatments. This means that all of the siphons remained flowing at the same capillary rise distance for long enough after any disturbance so that negligible change in flow rate was occurring. A preliminary experiment was completed earlier and provided experience for the time necessary to reach steady state.

A 4-inch diameter PVC pipe was used to construct a siphon similar to the experimental units described above. This siphon was filled with air-dried MichDOT 2NS sand which contained no particles larger than 3.36 mm in diameter and contained negligible amounts of fines. This siphon was filled and capped as previously described before being placed on a support structure with the upflow leg submerged in water. The siphon was allowed to run for thirty days before the flow volume was measured at a rise distance of 8 cm.

After this initial flow reading the water level was lowered by one centimeter to a rise distance of 9 cm. From this point in time flow volume readings were taken about every four hours for 10 days at a constant rise distance of 9 cm. The results of this experiment indicated that, after an initial decrease, the flow volume through the siphon reached a constant state after five days. Based on these findings the primary experimentation siphons were allowed to remain constantly running at a set rise distance for at least 5 days after each increase in the capillary rise distance.

Chapter 4

RESULTS AND DISCUSSION

Effective Size

Three different particle-size distributions of sand media were used to compare capillary flux over an impermeable barrier as a function of the media's effective size, or D_{10}. The effective sizes considered were 0.1 mm, 0.2 mm and 0.4 mm. The media distributions were all pre-determined and mixed so that a consistent uniformity coefficient of 2.5 was maintained across all three treatments. The capillary siphons were also packed to the same bulk density ($\rho_b = 1.6$ g/cm^3) in order to ensure consistent total pore volumes, thereby eliminating porosity as a variable between treatments.

These siphons were then subjected to the experimental procedure described elsewhere in this thesis, and data were collected according to the protocol defined therein. The resulting data are shown graphically in Figures 5, 6 and 7. Each of the data points shown in these figures is the average of nine individual measurements of system outflow: three replicate siphons for each treatment from which three consecutive outflow measurements were taken. Each data point is accompanied by bars which indicate the standard deviation of the nine averaged measurements.

The intermediate effective size ($D_{10} = 0.2$ mm) delivered the greatest outflow at all
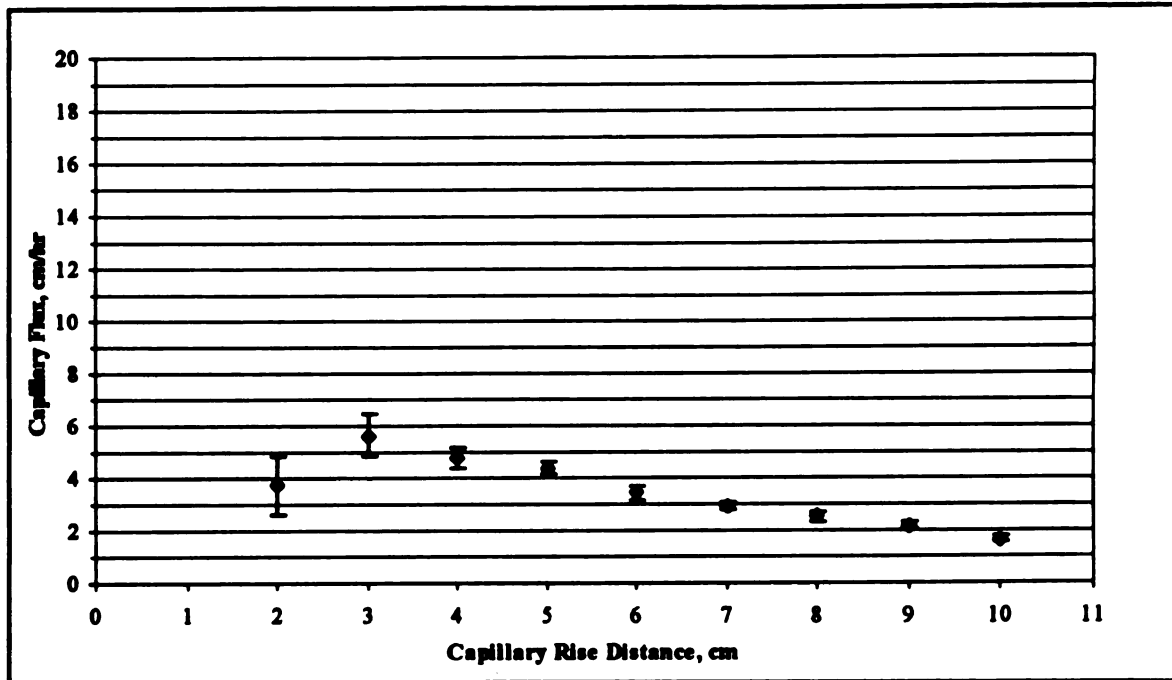
Figure 5. Mean steady-state capillary flux over an impermeable barrier at various rise distances with standard deviation bars (D_{10}= 0.1 mm; U= 2.5).

capillary rise distances (z) examined. The maximum averaged flux for this media was 15.5 cm/hr at z = 5 cm with a standard deviation (SD) of 2.94 cm/hr. The outflow from this intermediate media decreased to 4.9 cm/hr (SD = 0.54 cm/hr) at z = 10 cm. At z < 5 cm the measured outflow was found to decrease to 7.0 cm/hr (SD = 3.52 cm/hr) at z = 2.0 cm.

The smallest media examined (D_{10} = 0.1 mm) delivered the second highest flux values at all rise distances examined. The maximum outflow of this media was measured at z = 3 cm where the flux was 5.6 cm/hr (SD = 0.81 cm/hr). The outflow decreased to a minimum flow of 1.63 cm/hr (SD = 0.13 cm/hr) as z increased to 10 cm. The initial outflow at z = 2 cm was measured to be 3.8 cm/hr (SD = 1.09 cm/hr).

The capillary flux values were smallest at all rise distances for the largest media examined (D_{10} = 0.4 mm). These values ranged from 5.2 cm/hr (SD = 2.08 cm/hr) at z = 3
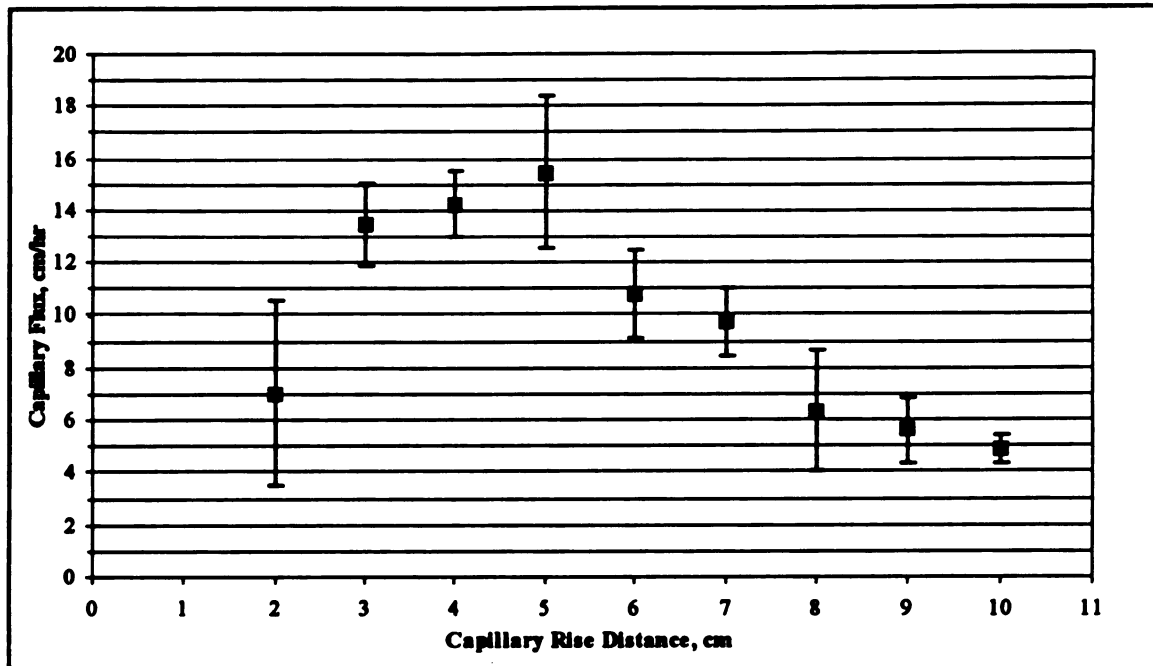
Figure 6. Mean steady-state capillary flux over an impermeable barrier at various rise distances with standard deviation bars (D_{10} = 0.2 mm; U = 2.5).

cm to a low of 0.2 cm/hr (SD = 0.11 cm/hr) at z = 10 cm. The flux at z = 2 cm was found to be 2.2 cm/hr with SD equal to 1.31 cm/hr.

It can be seen in Figures 5, 6 and 7 that the resultant flux at 2 cm rise distance is lower than the trend implied by the other data. Disinfectant was not added to the water supply until after the 2 cm data were measured. This is suspected to have resulted in inaccurately low flow rates at 2 cm due to the possible buildup of microorganisms in the media which could impede the flow of water by blocking some of the pore space pathways. Therefore these 2 cm data were not included in the following data analysis and discussion.

It is well acknowledged in the literature (Moore, 1939; Suter, 1964; Terzaghi and Peck, 1967; Hillel, 1982) that under typical saturated conditions the permeability should
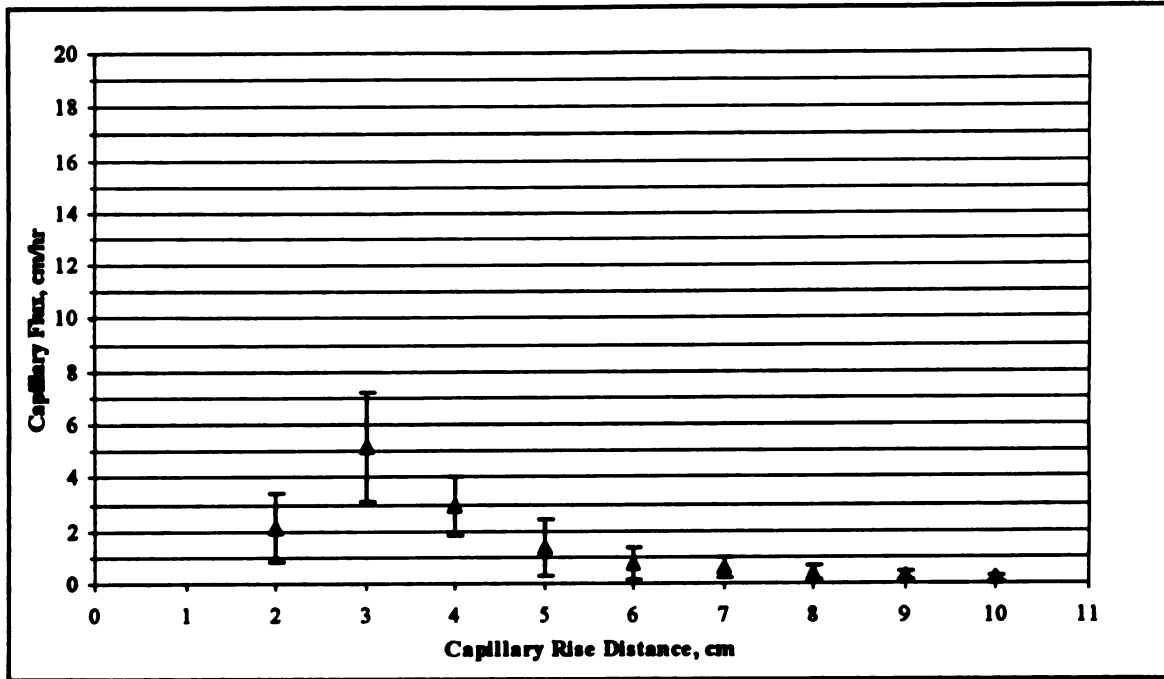
Figure 7. Mean steady-state capillary flux over an impermeable barrier at various rise distances with standard deviation bars (D_{10}= 0.4 mm; U = 2.5).

be greater for larger-grained media than for media made up of smaller grains, i.e. k_{coarse} >

k_{fine}. This can describe the movement of water over an impermeable barrier in porous

media from an upstream phreatic elevation greater than that of the barrier rim, to a

downstream water level below the rim elevation. As the upstream level is lowered to some

elevation below this rim, the flow system parameters change to those of an unsaturated

flow condition.

In this unsaturated flow condition the matric potential gradient of the media

becomes the dominant driving force for water movement rather than the gravitational

potential. Upward capillary flux has been examined by soil scientists (Alexander, 1982;

Malik et. al. 1989) in order to model the movement of water from a subsurface water table

to the root zone of plants, and/or to the ground surface where evaporation can take place.

As the water table elevation is lowered beyond some critical point, larger-grained media

(i.e. coarse sand) can move less water a given rise distance than a finer-grained material. This implies a cross-over in the Flux vs. Rise Distance curves for any two systems which vary only in the effective size of the media.

At a capillary rise distance equal to zero the flow over the barrier can be expected to be saturated as the tension-saturated zone, or capillary fringe, will extend to some elevation above the barrier. In this situation the coarse sand media (D_{10} = 0.4 mm) should provide the greatest outflow, followed sequentially by the intermediate (D_{10} = 0.2 mm) and fine sand (D_{10} = 0.1 mm). As the capillary rise distance is increased (by lowering the phreatic level upstream of the barrier), the system outflow will be controlled by the limiting zone of water movement. In unsaturated homogeneous media this can be expected to occur in the zone with the lowest moisture content. In the upflow leg of the siphon system this will be in the area of the barrier rim. The limiting flow for the overall system should occur in this upflow leg where the water must move against the gradient of gravitational potential.

The ability of any given media to transmit water decreases as air replaces the water in the pore space. This occurs first in the larger pores as the media is desaturated. A coarse-grained material will generally possess a greater proportion of large pores than will a finer material. The outflow from the coarser media will therefore drop off more rapidly as the rise distance is incrementally increased due to desaturation of the larger pores in the limiting flow zone. Conversely, the flow rate through the finer material will decrease more slowly over the same rise distance increase. Because fewer of these large pores exist in the fine media, their contribution to the total flow is smaller as the relative matric volume dewatered by the rise distance increase is less.

This means that the system outflow should be the same at some point for any two media of different effective sizes as they are changed from a saturated to an unsaturated or semi-saturated flow condition. Before this point the larger media (and associated large pores) will have greater outflow, while beyond this point the smaller media will have a greater proportion of pore space contributing to the flow and therefore the outflow will be greater (assuming that the porosity and other variables are kept constant).

Figure 8 represents exponential prediction curves generated from the Flux vs. Rise Distance data collected for the three different effective sizes. This graph confirms that the 0.4 mm effective size has the greatest initial slope (ie. change in flow vs. head), and the 0.1 mm media curve has the least slope. The graph also shows the cross-over points for the
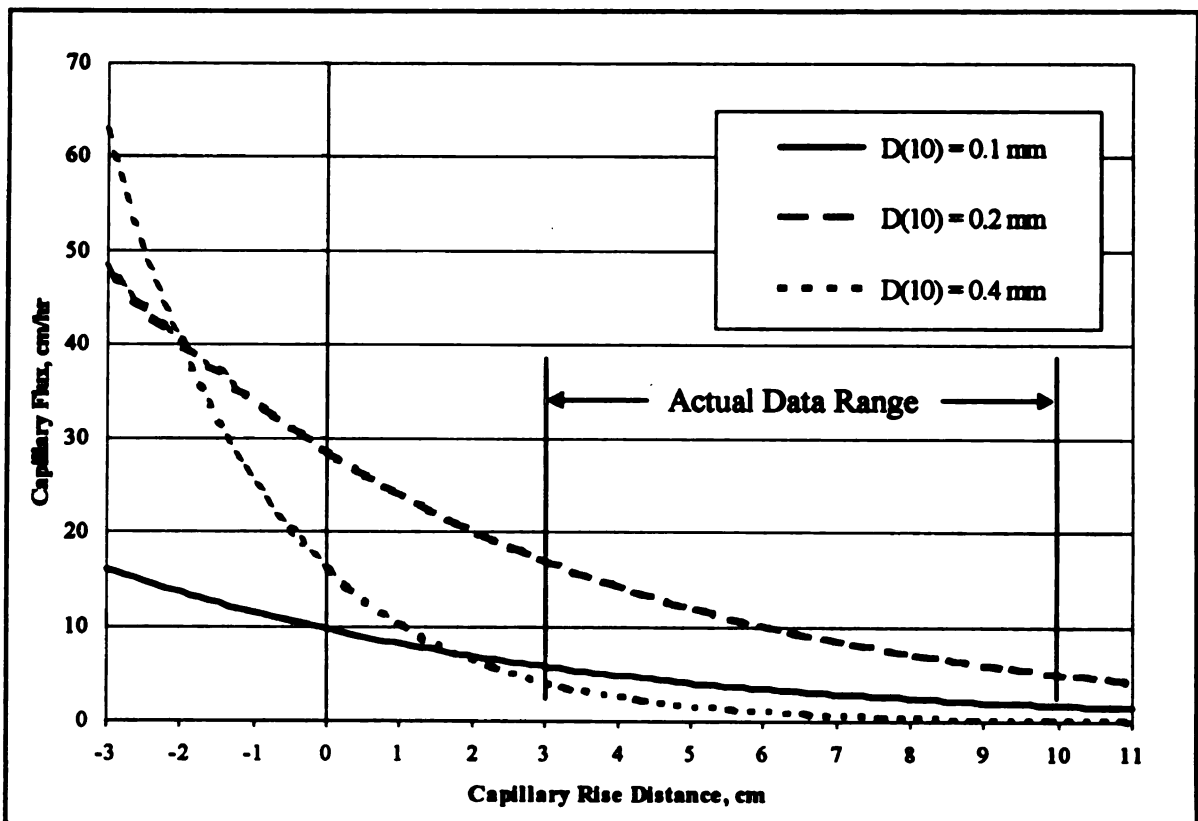
Figure 8. Exponential prediction curves from measured capillary flux of water through porous media of three different effective sizes ($U = 2.5$).

0.1 mm and 0.2 mm curves with the 0.4 mm curve. The corresponding cross-over point for the 0.1 mm and 0.2 mm curves should occur at some greater rise distance as expected from theory and literature related to capillary rise from finer media at greater distances.

The cross-over for the 0.2 mm and 0.4 mm media occurs at some small distance above the siphon invert as the transport media becomes saturated, given that the saturated hydraulic conductivity of larger media allows greater flow. The cross-over for the 0.1 mm and 0.4 mm media occurs while the system is nearly saturated and capillary fringe effects allow the flow rate of the larger media to increase more rapidly than the finer media. This graph supports the theory that media with an intermediate effective size can deliver the greatest system outflow over a specified range of capillary rise distances.

Results similar to these were indicated in the work of Ijjas (1965) and Malik et al. (1989) although under different experimental conditions. Ijjas measured the capillary discharge over an impermeable barrier for a medium (D_{10} = 0.13 mm) and a finer (D_{10} = 0.08 mm) grained sand at various rise distances. He reported that the capillary discharge curves crossed at an elevation slightly above the barrier, with the finer media delivering greater outflow as the rise distance was increased.

Malik et al. (1989) measured the maximal capillary rise as a function of height from the water table for a number of soils ranging from a sand to a silt clay loam. They reported that the slope of their curves decreased more steeply for coarse textured soils, and indicated cross-over points for these curves. While the range of heights from the water table studied by Malik and his colleagues were generally greater than 20 cm, the theoretical basis for their results was confirmed at smaller heights by Parlange et al. (1990) and is further confirmed empirically by this work.

Uniformity

The second part of this work was designed to examine the effect of grain size uniformity on capillary outflow from a siphon system. The uniformity coefficient U is a measure of the variation in grain sizes present in a given unconsolidated media system. Sand separates were mixed so that three different uniformities could be studied: 1.5, 2.5 and 4.5. A smaller value of U indicates a more uniform distribution of grain sizes. The effective size for all systems was kept the same (D_{10} = 0.2 mm), while bulk densities of 1.6 g/cm^3 were maintained. At the same effective size for all three mixes, a higher uniformity coefficient indicates more particles of larger size in the mix and likely some larger pores as well.

The most uniform media (U = 1.5) delivered the greatest outflow of 16.4 cm/hr (SD = 1.68 cm/hr) at a rise distance of 3 cm, but this was the only instance where this media exceeded both of the other treatments. The data for this treatment can be seen in Figure 9. The intermediate media (U = 2.5) generally delivered the highest outflows at rise distances of 4 cm and greater (see Figure 6). The least uniform media (U = 4.5) was found to deliver the least outflow at $z \geq 7$ cm and, as discussed later in this section, even these numbers may be artificially high. The data for this treatment can be seen in Figure 10.

The effect of media uniformity on capillary flux is not clearly evident from these results. This may be due to the fact that even distribution of particles within the U-shaped siphon is difficult to control, even under careful packing procedures. This is particularly true for the least uniform media which contains a wide range of particle sizes. These particles can end up in any number of various configurations which may have a great effect
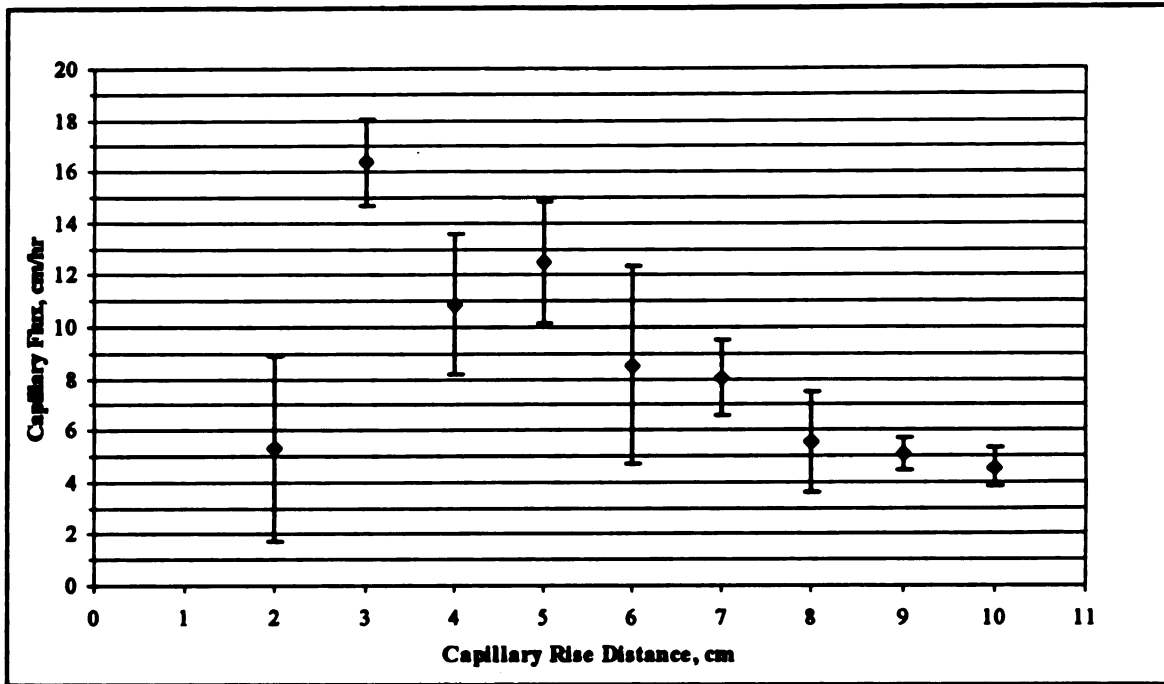
Figure 9. Mean steady-state capillary flux over an impermeable barrier at various rise distances with standard deviation bars $(D_{10} = 0.2$ mm; $U = 1.5)$.

upon the performance of the system. For example, the pore space can be radically different depending upon whether the smaller particles find their way into the spaces between the larger particles. This would lead to smaller average pore sizes and a more uniform pore-size distribution, thereby affecting capillary rise.

Evidence of this effect can be seen in the large variability in measured outflows of the three siphons containing the least uniform media $(U = 4.5)$. The standard deviations for this treatment range from 38% to 83% of the mean flux values with the majority greater than 50% of the mean. This is due to the measured outflow of one of the three treatment siphons which consistently delivered more than twice the outflow of the other two. If this individual siphon is excluded, the standard deviations for this treatment range from 2% to 23% of the mean for the data being analyzed. In this case the least uniform
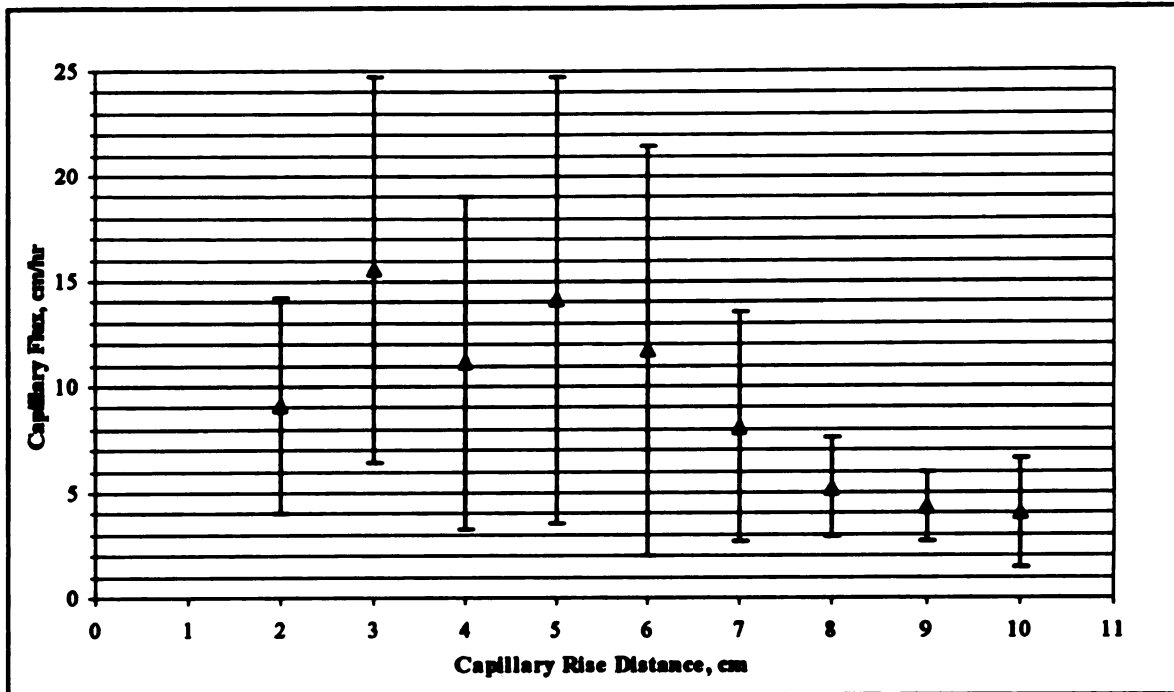
Figure 10. Mean steady-state capillary flux over an impermeable barrier at various rise distances with standard deviation bars (D_{10}= 0.2 mm; U = 4.5).

media system consistently delivered the lowest outflows for $z \geq 3$ cm. This adjusted data is shown in Figure 11.

Application of Results

The results stated and discussed above can help in a better understanding of the effects of some media parameters on capillary movement of water over an impermeable barrier in porous media. This information can be helpful to the study of upward movement from a water table to construction foundations, plant roots or the ground surface. The data is even more relevant when applied to systems which utilize flow over an impermeable vertical barrier.

In the case of water retention structures, such as canals and dikes, the goal is typically to minimize the flow over the barrier. For this situation it appears that a larger
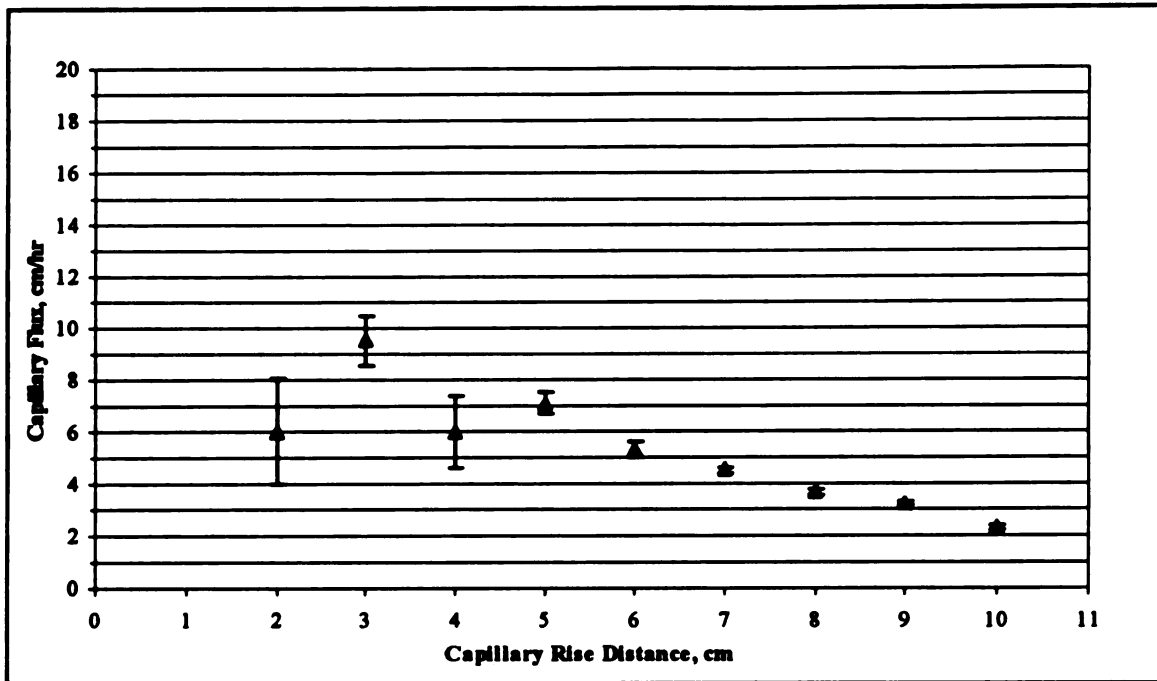
Figure 11. Adjusted mean steady-state capillary flux over an impermeable barrier at various rise distances with standard deviation bars (D_{10} = 0.2 mm; U = 4.5).

media effective size should minimize outflow, particularly if the vertical distance from the free water surface to the barrier rim is maximized. The data appears to indicate that outflow may also be minimized if the media particle sizes vary over a large range, although this result should be confirmed by further research.

Another important application of these results is the use of unsaturated flow over a barrier to create an aerobic phase in an upflow filter for wastewater treatment. In this case the goal is more likely to maximize the movement of the fluid over a barrier or to provide an appropriate residence time in an aerobic zone. This is in fact the application which instigated this research, specifically the range of rise distances and the media size which were investigated. Of course, there would be a number of other variables which would apply to that application which were not included in this study. Primary among these would be the use of wastewater instead of distilled water as the transported fluid.

Wastewater contains numerous constituents which could affect surface tension characteristics, pore clogging by suspended solids, the buildup of a biological layer on the media matrix, and other factors. To maximize system outflow, the data support the use of an intermediate particle size ($D_{10} \approx 0.2$ mm) at a rise distance which ranges from 3 to 5 cm. The data also seem to support the use of a fairly uniform media distribution ($U \approx 2.5$) to maximize outflow, although this was not definitively supported and needs further study.

Chapter 5

SUMMARY AND CONCLUSIONS

The phenomenon of capillary siphoning was studied and experimentation designed and executed to obtain data which could be used to better understand and quantify this process. Capillary siphoning has been defined as the natural transport due to capillary forces of a fluid over an impermeable barrier in unsaturated media. In this case the fluid was distilled, disinfected water, and the media was unconsolidated sand.

The primary impetus for this work was the use of capillary siphoning in the aerobic treatment zone of a decentralized wastewater treatment system which has recently been developed. This system relies upon capillary action to raise partially treated water up from a phreatic surface and into the unsaturated zone for final treatment before discharge. In order for the treated water to exit the system it must move up and over an impermeable barrier. It is this capillary rise and horizontal movement through the unsaturated media which provides the aerobic treatment.

The media which is contained in this portion of the treatment system should be chosen so that it provides adequate hydraulic capacity in addition to proper treatment. The capillary siphoning process must be able to discharge the volume of influent to the system while maintaining aerobic capillary flow without the barrier perimeter being excessive.

70

This can be achieved by choosing the optimal media based upon its capillary hydraulic characteristics. The primary goal of this work was to determine how the effective size and uniformity of the media particles influence the capillary discharge, and to quantify the flow rates which can be expected through these media over a range of rise distances.

The steady state capillary flux through media with three different effective sizes— 0.1 mm, 0.2 mm and 0.4 mm—was measured in the laboratory. Measurements were obtained at capillary rise distances ranging from 2 to 10 cm. The greatest outflow at all rise distances was obtained from the intermediate (0.2 mm) treatment. The maximum flux was 15.5 cm/hr at 5 cm rise distance for this media, decreasing to 4.9 cm/hr at 10 cm. This was greater than both of the other treatments which ranged from 5.6 cm/hr at 3 cm to 1.63 cm/hr at 10 cm for the 0.1 mm treatment, and from 5.2 cm/hr at 3 cm to 0.2 cm/hr at 10 cm for the 0.4 mm treatment.

The larger media can be expected to show the greatest outflow under saturated conditions due to its higher hydraulic conductivity, although once the transition is made to an unsaturated state the larger pores associated with this media will desaturate rapidly at small values of matric tension. This causes a sharp decline in the slope of the rise distance-capillary flux curve with a large percentage of the effective pore space making little contribution to flow even at small rise distances. This decline can be seen in the 85% decrease in flux as the rise distance was increased from 3 cm to 6 cm.

On the other hand, the smallest media studied will have the lowest saturated hydraulic conductivity, but as the media desaturates with increased rise distance a larger percentage of pores will continue to contribute to flow. Therefore the slope will decline at a slower rate, indicated by the less than 40% decrease in flux over the same range.

Therefore, media with an intermediate size can be expected to provide greater capillary discharge at these shallow rise distances. This is because it will have a greater conductivity at saturation than the smaller media, and decrease less rapidly with increased suction than the larger media. This was confirmed by the data collected in the laboratory, although further testing would be needed to determine whether the intermediate grain size selected—0.2 mm with a uniformity coefficient of 2.5—is the precise optimal size.

In the experiments conducted with uniformity as the variable, differences were not as apparent. Media having an effective size of 0.2 mm were prepared with three different coefficients of uniformity—1.5, 2.5 and 4.5. The capillary rise distances ranged from 2 cm to 10 cm. The most uniform media delivered the greatest flux: 16.4 cm/hr at a rise distance of 3 cm, decreasing to 4.6 cm/hr at 10 cm. The intermediate media ranged from 15.5 cm/hr at 5 cm to 4.3 cm/hr at 10 cm, while the least uniform media ranged from 15.6 cm/hr at 3 cm to 4.0 cm/hr at 10 cm of capillary rise. It should be noted that there was a great deal of variability in the readings of the individual treatment replicates for the least uniform media.

As the results above imply, it is difficult to determine how particle uniformity influences the capillary hydraulics of this granular porous media. The pore space contained within a uniform media can also be expected to be fairly uniform, with the extreme case being a media made up of identical spheres. As particle size variability is increased, a greater chance exists for smaller particles to fill in the larger spaces between particles. This introduces packing as a crucial variable in media with less uniformity, with the possibility of widely differing pore space configurations contained within replicates of similar media.

In conclusion, the objectives of this research as stated above have been met. The capillary flux at rise distances between 2 and 10 cm has been quantified for a number of different media mixtures. The influence of media effective size on flow rate at these rise distances has been studied, and a conclusion drawn regarding the importance of selecting the proper intermediate size for maximum flow. The influence of media uniformity on flow rate has also been studied. While no definitive conclusions could be drawn from the experimental data collected, results suggest that the variability of packing could be a significant factor affecting the flux through a system containing a wide range in particle sizes.

Further research needs to be done to extend this work to examine how media size and uniformity affect the transport of wastewater. The long term effects of capillary movement of wastewater through sand media should be researched, with particular emphasis on changes in the pore space. The effect of media packing on fluid transport also needs to be studied, particularly for less uniform media.

APPENDICES

APPENDIX A

Capillary Flux Laboratory Data for Siphon Set 0125 ($D_{10} = 0.1$ mm $U = 2.5$).

Capillary rise, cm		Capillary Flux, cm/hr					
		Siphon A	Siphon B	Siphon C	Average	Minimum	Maximum
2	Run #1	3.076	3.809	5.108	3.998	3.076	5.108
	Run #2	2.645	3.839	5.375	3.953	2.645	5.375
	Run #3	2.134	3.252	4.509	3.298	2.134	4.509
	Average	2.618	3.633	4.997	3.750		
	Minimum	2.134	3.252	4.509		2.134	
	Maximum	3.076	3.839	5.375			5.375
3	Run #1	4.639	5.896	6.397	5.644	4.639	6.397
	Run #2	4.526	5.847	6.264	5.545	4.526	6.264
	Run #3	4.560	6.023	6.443	5.675	4.560	6.443
	Average	4.575	5.922	6.368	5.622		
	Minimum	4.526	5.847	6.264		4.526	
	Maximum	4.639	6.023	6.443			6.443
4	Run #1	4.450	4.920	5.309	4.893	4.450	5.309
	Run #2	4.095	4.563	4.854	4.504	4.095	4.854
	Run #3	4.386	4.923	5.183	4.830	4.386	5.183
	Average	4.310	4.802	5.115	4.743		
	Minimum	4.095	4.563	4.854		4.095	
	Maximum	4.450	4.923	5.309			5.309
5	Run #1	4.288	4.170	4.574	4.344	4.170	4.574
	Run #2	4.499	4.443	4.789	4.577	4.443	4.789
	Run #3	4.214	4.141	4.533	4.296	4.141	4.533
	Average	4.334	4.251	4.632	4.406		
	Minimum	4.214	4.141	4.533		4.141	
	Maximum	4.499	4.443	4.789			4.789
6	Run #1	3.065	3.324	3.686	3.359	3.065	3.686
	Run #2	3.164	3.418	3.779	3.454	3.164	3.779
	Run #3	3.253	3.455	3.838	3.515	3.253	3.838
	Average	3.161	3.399	3.768	3.443		
	Minimum	3.065	3.324	3.686		3.065	
	Maximum	3.253	3.455	3.838			3.838

APPENDIX A

Capillary Flux Laboratory Data for Siphon Set 0125 (D_{10} = 0.1 mm U = 2.5) - cont.

Capillary rise, cm		Capillary Flux, cm/hr					
		Siphon A	Siphon B	Siphon C	Average	Minimum	Maximum
7	Run #1	2.822	2.813	3.167	2.934	2.813	3.167
	Run #2	2.815	2.817	3.144	2.925	2.815	3.144
	Run #3	2.835	2.828	3.169	2.944	2.828	3.169
	Average	2.824	2.820	3.160	2.934		
	Minimum	2.815	2.813	3.144		2.813	
	Maximum	2.835	2.828	3.169			3.169
8	Run #1	2.441	2.470	2.826	2.579	2.441	2.826
	Run #2	2.372	2.391	2.719	2.494	2.372	2.719
	Run #3	2.390	2.388	2.733	2.504	2.388	2.733
	Average	2.401	2.417	2.759	2.526		
	Minimum	2.372	2.388	2.719		2.372	
	Maximum	2.441	2.470	2.826			2.826
9	Run #1	2.151	2.042	2.369	2.187	2.042	2.369
	Run #2	2.138	2.055	2.368	2.187	2.055	2.368
	Run #3	2.164	2.052	2.362	2.192	2.052	2.362
	Average	2.151	2.049	2.366	2.189		
	Minimum	2.138	2.042	2.362		2.042	
	Maximum	2.164	2.055	2.369			2.369
10	Run #1	1.621	1.492	1.795	1.636	1.492	1.795
	Run #2	1.618	1.494	1.778	1.630	1.494	1.778
	Run #3	1.627	1.492	1.794	1.638	1.492	1.794
	Average	1.622	1.493	1.789	1.635		
	Minimum	1.618	1.492	1.778		1.492	
	Maximum	1.627	1.494	1.795			1.795

APPENDIX B

APPENDIX B

Capillary Flux Laboratory Data for Siphon Set 0225 (D_{10} = 0.2 mm U = 2.5).

Capillary rise, cm		Capillary Flux, cm/hr Siphon A	Siphon B	Siphon C	Average	Minimum	Maximum
2	Run #1	4.308	7.125	11.719	7.717	4.308	11.719
	Run #2	3.300	6.918	11.774	7.331	3.300	11.774
	Run #3	2.341	5.675	10.103	6.040	2.341	10.103
	Average	3.316	6.573	11.199	7.029		
	Minimum	2.341	5.675	10.103		2.341	
	Maximum	4.308	7.125	11.774			11.774
3	Run #1	12.426	13.121	15.489	13.679	12.426	15.489
	Run #2	11.640	12.906	15.079	13.208	11.640	15.079
	Run #3	11.421	13.268	15.594	13.428	11.421	15.594
	Average	11.829	13.099	15.387	13.438		
	Minimum	11.421	12.906	15.079		11.421	
	Maximum	12.426	13.268	15.594			15.594
4	Run #1	16.483	13.379	14.495	14.786	13.379	16.483
	Run #2	14.855	12.635	13.482	13.658	12.635	14.855
	Run #3	15.704	13.259	14.015	14.326	13.259	15.704
	Average	15.681	13.091	13.997	14.257		
	Minimum	14.855	12.635	13.482		12.635	
	Maximum	16.483	13.379	14.495			16.483
5	Run #1	19.406	12.045	14.874	15.442	12.045	19.406
	Run #2	19.470	12.679	15.733	15.961	12.679	19.470
	Run #3	17.862	12.032	14.990	14.961	12.032	17.862
	Average	18.912	12.252	15.199	15.455		
	Minimum	17.862	12.032	14.874		12.032	
	Maximum	19.470	12.679	15.733			19.470
6	Run #1	8.933	9.615	12.352	10.300	8.933	12.352
	Run #2	9.809	10.577	13.485	11.290	9.809	13.485
	Run #3	9.289	10.036	12.793	10.706	9.289	12.793
	Average	9.344	10.076	12.877	10.765		
	Minimum	8.933	9.615	12.352		8.933	
	Maximum	9.809	10.577	13.485			13.485

76

APPENDIX B

Capillary Flux Laboratory Data for Siphon Set 0225 (D_{10} = 0.2 mm U = 2.5) - cont.

Capillary rise, cm		Capillary Flux, cm/hr					
		Siphon A	Siphon B	Siphon C	Average	Minimum	Maximum
7	Run #1	11.271	8.111	10.145	9.843	8.111	11.271
	Run #2	11.008	8.067	10.057	9.711	8.067	11.008
	Run #3	10.829	8.053	10.119	9.667	8.053	10.829
	Average	11.036	8.077	10.107	9.740		
	Minimum	10.829	8.053	10.057		8.053	
	Maximum	11.271	8.111	10.145			11.271
8	Run #1	3.489	7.073	8.895	6.486	3.489	8.895
	Run #2	3.380	6.854	8.652	6.295	3.380	8.652
	Run #3	3.337	6.808	8.615	6.253	3.337	8.615
	Average	3.402	6.911	8.721	6.345		
	Minimum	3.337	6.808	8.615		3.337	
	Maximum	3.489	7.073	8.895			8.895
9	Run #1	4.116	5.794	7.033	5.648	4.116	7.033
	Run #2	4.005	5.780	6.929	5.571	4.005	6.929
	Run #3	4.002	5.790	6.912	5.568	4.002	6.912
	Average	4.041	5.788	6.958	5.596		
	Minimum	4.002	5.780	6.912		4.002	
	Maximum	4.116	5.794	7.033			7.033
10	Run #1	4.885	4.298	5.564	4.916	4.298	5.564
	Run #2	4.769	4.308	5.532	4.870	4.308	5.532
	Run #3	4.660	4.323	5.536	4.839	4.323	5.536
	Average	4.771	4.310	5.544	4.875		
	Minimum	4.660	4.298	5.532		4.298	
	Maximum	4.885	4.323	5.564			5.564

APPENDIX C

APPENDIX C

Capillary Flux Laboratory Data for Siphon Set 0425 ($D_{10} = 0.4$ mm $U = 2.5$).

Capillary rise, cm		Capillary Flux, cm/hr					
		Siphon A	Siphon B	Siphon C	Average	Minimum	Maximum
2	Run #1	1.249	4.187	1.987	2.474	1.249	4.187
	Run #2	0.825	3.869	1.847	2.180	0.825	3.869
	Run #3	0.605	3.225	1.562	1.797	0.605	3.225
	Average	0.893	3.760	1.799	2.151		
	Minimum	0.605	3.225	1.562		0.605	
	Maximum	1.249	4.187	1.987			4.187
3	Run #1	2.507	5.687	7.105	5.100	2.507	7.105
	Run #2	2.439	5.770	7.013	5.074	2.439	7.013
	Run #3	2.569	6.223	7.277	5.356	2.569	7.277
	Average	2.505	5.893	7.132	5.177		
	Minimum	2.439	5.687	7.013		2.439	
	Maximum	2.569	6.223	7.277			7.277
4	Run #1	1.721	2.831	4.371	2.975	1.721	4.371
	Run #2	1.718	2.656	4.076	2.817	1.718	4.076
	Run #3	1.833	2.818	4.334	2.995	1.833	4.334
	Average	1.757	2.768	4.260	2.929		
	Minimum	1.718	2.656	4.076		1.718	
	Maximum	1.833	2.831	4.371			4.371
5	Run #1	0.538	0.752	2.736	1.342	0.538	2.736
	Run #2	0.604	0.829	2.903	1.446	0.604	2.903
	Run #3	0.645	0.762	2.732	1.380	0.645	2.732
	Average	0.595	0.781	2.790	1.389		
	Minimum	0.538	0.752	2.732		0.538	
	Maximum	0.645	0.829	2.903			2.903
6	Run #1	0.420	0.309	1.562	0.764	0.309	1.562
	Run #2	0.428	0.323	1.563	0.771	0.323	1.563
	Run #3	0.429	0.317	1.555	0.767	0.317	1.555
	Average	0.425	0.316	1.560	0.767		
	Minimum	0.420	0.309	1.555		0.309	
	Maximum	0.429	0.323	1.563			1.563

APPENDIX C

Capillary Flux Laboratory Data for Siphon Set 0425 (D_{10} = 0.4 mm U = 2.5) - cont.

Capillary rise, cm		Capillary Flux, cm/hr			Average	Minimum	Maximum
		Siphon A	Siphon B	Siphon C			
7	Run #1	0.537	0.264	1.126	0.642	0.264	1.126
	Run #2	0.533	0.259	1.105	0.632	0.259	1.105
	Run #3	0.543	0.252	1.119	0.638	0.252	1.119
	Average	0.538	0.258	1.117	*0.638*		
	Minimum	0.533	0.252	1.105		**0.252**	
	Maximum	0.543	0.264	1.126			**1.126**
8	Run #1	0.368	0.145	0.734	0.416	0.145	0.734
	Run #2	0.364	0.153	0.732	0.416	0.153	0.732
	Run #3	0.365	0.143	0.725	0.411	0.143	0.725
	Average	0.366	0.147	0.730	*0.414*		
	Minimum	0.364	0.143	0.725		**0.143**	
	Maximum	0.368	0.153	0.734			**0.734**
9	Run #1	0.272	0.126	0.505	0.301	0.126	0.505
	Run #2	0.285	0.132	0.505	0.307	0.132	0.505
	Run #3	0.277	0.132	0.501	0.303	0.132	0.501
	Average	0.278	0.130	0.504	*0.304*		
	Minimum	0.272	0.126	0.501		**0.126**	
	Maximum	0.285	0.132	0.505			**0.505**
10	Run #1	0.186	0.079	0.317	0.194	0.079	0.317
	Run #2	0.187	0.083	0.310	0.193	0.083	0.310
	Run #3	0.192	0.066	0.332	0.197	0.066	0.332
	Average	0.188	0.076	0.320	*0.195*		
	Minimum	0.186	0.066	0.310		**0.066**	
	Maximum	0.192	0.083	0.332			**0.332**

APPENDIX D

APPENDIX D

Capillary Flux Laboratory Data for Siphon Set 0215 (D_{10} = 0.2 mm U = 1.5).

Capillary rise, cm		Capillary Flux, cm/hr			Average	Minimum	Maximum
		Siphon A	Siphon B	Siphon C			
2	Run #1	1.109	6.758	9.845	5.904	1.109	9.845
	Run #2	0.957	6.048	9.429	5.478	0.957	9.429
	Run #3	0.823	4.909	7.988	4.573	0.823	7.988
	Average	0.963	5.905	9.088	5.319		
	Minimum	0.823	4.909	7.988		0.823	
	Maximum	1.109	6.758	9.845			9.845
3	Run #1	17.568	17.927	14.323	16.606	14.323	17.927
	Run #2	17.033	17.962	14.208	16.401	14.208	17.962
	Run #3	16.911	17.520	14.070	16.167	14.070	17.520
	Average	17.171	17.803	14.200	16.391		
	Minimum	16.911	17.520	14.070		14.070	
	Maximum	17.568	17.962	14.323			17.962
4	Run #1	9.522	14.921	9.765	11.403	9.522	14.921
	Run #2	8.264	13.765	8.997	10.342	8.264	13.765
	Run #3	8.542	14.565	9.647	10.918	8.542	14.565
	Average	8.776	14.417	9.470	10.888		
	Minimum	8.264	13.765	8.997		8.264	
	Maximum	9.522	14.921	9.765			14.921
5	Run #1	12.700	15.303	9.832	12.612	9.832	15.303
	Run #2	13.064	15.994	10.568	13.209	10.568	15.994
	Run #3	11.377	14.165	9.489	11.677	9.489	14.165
	Average	12.380	15.154	9.963	12.499		
	Minimum	11.377	14.165	9.489		9.489	
	Maximum	13.064	15.994	10.568			15.994
6	Run #1	7.086	12.579	4.366	8.010	4.366	12.579
	Run #2	7.897	14.129	5.059	9.029	5.059	14.129
	Run #3	7.371	13.312	4.748	8.477	4.748	13.312
	Average	7.451	13.340	4.724	8.505		
	Minimum	7.086	12.579	4.366		4.366	
	Maximum	7.897	14.129	5.059			14.129

APPENDIX D

Capillary Flux Laboratory Data for Siphon Set 0215 (D_{10} = 0.2 mm U = 1.5) - cont.

Capillary rise, cm		Capillary Flux, cm/hr Siphon A	Siphon B	Siphon C	Average	Minimum	Maximum
7	Run #1	7.832	9.911	6.504	8.082	6.504	9.911
	Run #2	7.747	9.877	6.564	8.063	6.564	9.877
	Run #3	7.558	9.798	6.578	7.978	6.578	9.798
	Average	7.712	9.862	6.549	8.041		
	Minimum	7.558	9.798	6.504		6.504	
	Maximum	7.832	9.911	6.578			9.911
8	Run #1	3.464	8.039	5.713	5.739	3.464	8.039
	Run #2	3.288	7.701	5.509	5.499	3.288	7.701
	Run #3	3.242	7.732	5.503	5.492	3.242	7.732
	Average	3.331	7.824	5.575	5.577		
	Minimum	3.242	7.701	5.503		3.242	
	Maximum	3.464	8.039	5.713			8.039
9	Run #1	4.810	5.932	4.446	5.063	4.446	5.932
	Run #2	4.730	5.880	4.675	5.095	4.675	5.880
	Run #3	4.654	5.870	4.746	5.090	4.654	5.870
	Average	4.731	5.894	4.622	5.082		
	Minimum	4.654	5.870	4.446		4.446	
	Maximum	4.810	5.932	4.746			5.932
10	Run #1	4.908	5.218	3.495	4.540	3.495	5.218
	Run #2	4.885	5.229	3.580	4.565	3.580	5.229
	Run #3	4.866	5.237	3.645	4.583	3.645	5.237
	Average	4.887	5.228	3.574	4.563		
	Minimum	4.866	5.218	3.495		3.495	
	Maximum	4.908	5.237	3.645			5.237

APPENDIX E

APPENDIX E

Capillary Flux Laboratory Data for Siphon Set 0245 (D_{10} = 0.2 mm U = 4.5).

Capillary rise, cm		Capillary Flux, cm/hr					
		Siphon A	Siphon B	Siphon C	Average	Minimum	Maximum
2	Run #1	6.973	17.078	7.763	10.604	6.973	17.078
	Run #2	4.257	16.182	7.640	9.360	4.257	16.182
	Run #3	2.785	12.840	6.658	7.428	2.785	12.840
	Average	4.672	15.367	7.354	9.131		
	Minimum	2.785	12.840	6.658		2.785	
	Maximum	6.973	17.078	7.763			17.078
3	Run #1	8.999	28.617	10.443	16.020	8.999	28.617
	Run #2	8.618	27.469	10.238	15.442	8.618	27.469
	Run #3	8.338	27.142	10.438	15.306	8.338	27.142
	Average	8.652	27.743	10.373	15.589		
	Minimum	8.338	27.142	10.238		8.338	
	Maximum	8.999	28.617	10.443			28.617
4	Run #1	4.828	21.665	7.206	11.233	4.828	21.665
	Run #2	4.545	20.949	7.008	10.834	4.545	20.949
	Run #3	4.865	22.120	7.509	11.498	4.865	22.120
	Average	4.746	21.578	7.241	11.188		
	Minimum	4.545	20.949	7.008		4.545	
	Maximum	4.865	22.120	7.509			22.120
5	Run #1	7.144	27.499	6.418	13.687	6.418	27.499
	Run #2	7.594	28.821	6.919	14.445	6.919	28.821
	Run #3	7.487	28.434	6.940	14.287	6.940	28.434
	Average	7.408	28.252	6.759	14.140		
	Minimum	7.144	27.499	6.418		6.418	
	Maximum	7.594	28.821	6.940			28.821
6	Run #1	4.866	23.198	5.045	11.036	4.866	23.198
	Run #2	5.462	26.121	5.725	12.436	5.462	26.121
	Run #3	5.182	24.628	5.378	11.729	5.182	24.628
	Average	5.170	24.649	5.383	11.734		
	Minimum	4.866	23.198	5.045		4.866	
	Maximum	5.462	26.121	5.725			26.121

APPENDIX E

Capillary Flux Laboratory Data for Siphon Set 0245 ($D_{10} = 0.2$ mm $U = 4.5$) - cont.

Capillary rise, cm		Capillary Flux, cm/hr			Average	Minimum	Maximum
		Siphon A	Siphon B	Siphon C			
7	Run #1	4.515	15.352	4.397	8.088	4.397	15.352
	Run #2	4.616	15.517	4.494	8.209	4.494	15.517
	Run #3	4.556	15.129	4.435	8.040	4.435	15.129
	Average	4.562	15.333	4.442	8.112		
	Minimum	4.515	15.129	4.397		4.397	
	Maximum	4.616	15.517	4.494			15.517
8	Run #1	3.535	8.396	3.779	5.236	3.535	8.396
	Run #2	3.544	8.338	3.780	5.221	3.544	8.338
	Run #3	3.524	8.403	3.783	5.237	3.524	8.403
	Average	3.534	8.379	3.781	5.231		
	Minimum	3.524	8.338	3.779		3.524	
	Maximum	3.544	8.403	3.783			8.403
9	Run #1	3.259	6.551	3.170	4.327	3.170	6.551
	Run #2	3.290	6.575	3.193	4.353	3.193	6.575
	Run #3	3.282	6.448	3.172	4.301	3.172	6.448
	Average	3.277	6.525	3.178	4.327		
	Minimum	3.259	6.448	3.170		3.170	
	Yaximum	3.290	6.575	3.193			6.575
10	Run #1	2.358	7.525	2.269	4.051	2.269	7.525
	Run #2	2.338	7.526	2.277	4.047	2.277	7.526
	Run #3	2.336	7.445	2.272	4.017	2.272	7.445
	Average	2.344	7.499	2.273	4.038		
	Minimum	2.336	7.445	2.269		2.269	
	Maximum	2.358	7.526	2.277			7.526

LIST OF REFERENCES

LIST OF REFERENCES

Alexander, L. 1982. Predicted Steady Upward Flux from the Water Table. MS Thesis North Carolina State University, Raleigh.

Anat, A., H. R. Duke and A. T. Corey. 1965. Steady Upward Flow from Water Tables. Hydrology Paper #7. Colorado State Univ. Ft. Collins, Colorado.

Baver, L. D. 1956. Soil Physics. 3rd Edition. John Wiley and Sons, New York.

Bear, J. 1979. Hydraulics of Groundwater. McGraw-Hill, New York.

Brooks, R. H. and A. T. Corey. 1964. Hydraulic Properties of Porous Media. Hydrology Paper #3. Colorado State Univ. Ft. Collins, Colorado.

Carman, P. C. 1941. Capillary Rise and Capillary Movement of Moisture in Fine Sands. Soil Sci. 34:1-14.

Corey, A. T. 1977. Mechanics of Heterogenous Fluids in Porous Media. Water Resources Publications, Ft. Collins, Colorado.

Corey, A. T. 1986. Mechanics of Immiscible Fluids in Porous Media. 2nd Edition. Water Resources Publications, Littleton, Colorado.

Dullien, F. A. L. 1972. Pore Structure and Flow Properties of Porous Media. *In* Proceedings of the Second Symposium on Fundamentals of Transport Phenomena in Porous Media I:58-73.

Eastburn, R. P. and W. F. Ritter. 1985. Denitrification in On-Site Wastewater Treatment Systems—A Review. *In* On-Site Wastewater Treatment; Proceedings of the Fourth National Symposium on Individual and Small Community Sewage Systems. ASAE. 305-313.

Freeze, R. A. 1969. The Mechanism of Natural Ground-water Recharge and Discharge 1. One-dimensional, Vertical, Unsteady, Unsaturated Flow above a Recharging or Discharging Ground-water Flow System. Water Resources Res. 5:153-171.

Freeze, R. A. and J. A. Cherry. 1979. Groundwater. Prentice-Hall, New Jersey.

Gardner, W. R. 1958. Some Steady State Solutions of the Unsaturated Moisture Flow Equation with Application to Evaporation from a Water Table. Soil Sci. 85:228-232.

Hillel, D. 1982. Introduction to Soil Physics. Academic Press, New York.

Ijjas, I. 1965. Capillary Losses in Irrigation Canals. Hidrologiai Kozlony, 7:295-308. (Hungarian; Summary in English)

Ijjas, I. 1966. Effect of Compactness and Initial Moisture Content of the Soil on the Process of Capillary Rise. UNESCO Symposium on Water in the Unsaturated Zone. II:547-559.

Klute, A. 1952. Some Theoretical Aspects of the Flow of Water in Unsaturated Materials. Soil Sci. Soc. Am. Proc. 16:144-148.

Kumar, S. and R. S. Malik. 1990. Verification of Quick Capillary Rise Approach for Determining Pore Geometric Characteristics in Soils of Varying Texture. Soil Sci. 150:883-888.

Laak, R. 1982. On-Site Soil Systems, Nitrogen Removal. In Alternative Wastewater Treatment. Low-Cost Small Systems, Research and Development. Eds. A. S. Eikum and R. W. Seabloom. D. Reidel Publishing Co., Boston.

Lambe, T. W. and R. V. Whitman. 1969. Soil Mechanics. John Wiley and Sons, Inc., New York.

Laliberte, G. E. and R. H. Brooks. 1967. Hydraulic Properties of Disturbed Soil Materials Affected by Porosity. Soil Sci. Soc. Am. Proc. 31:451-454.

Laroussi, C. and L. W. De Backer. 1979. Relation Between Geometrical Properties of Glass Beads Media and their Main $\psi(\theta)$ Hysteresis Loops. Soil Sci. Soc. Am. J. 43:646-650.

Lawrence, G. P. 1977. Measurement of Pore Sizes in Fine-Textured Soils: A Review of Existing Techniques. J. of Soil Sci. 28:527-540.

Malik, R. S., S. Kumar and I. S. Dahiya. 1984. An Approach to Quick Determination of Some Water Transmission Characteristics of Porous Media. Soil Sci. 137:395-400.

Malik, R. S., S. Kumar and R. K. Malik. 1989. Maximum Capillary Rise Flux as a Function of Height from the Water Table. Soil Sci. 148:322-326.

Miller, R. D. and E. E. Miller. 1955. Theory of Capillary Flow: II. Experimental Information. Soil Sci. Soc. Am. Proc. 19:271-275.

Moore, R. E. 1939. Water Conduction from Shallow Water Tables. Hilgardia. 12:383-426.

Morel-Seytoux, H. J. 1969. Introduction to Flow of Immiscible Liquids in Porous Media. In Flow Through Porous Media. Ed. R. J. M. De Wiest. Academic Press, New York. 456-515.

Novak, L. J. 1972. Transport Phenomena in Porous Media with Emphasis on Water Movement in Soils. Ph.D. Thesis. Michigan State University. East Lansing, MI.

Otis, R. J. 1985. Soil Clogging: Mechanisms and Control. In On-Site Wastewater Treatment; Proceedings of the Fourth National Symposium on Individual and Small Community Sewage Systems. ASAE. 238-250.

Parlange, J. -Y. 1980. Water Transport in Soils. Annu. Rev. Fluid Mech. 12:77-102.

Parlange, J. -Y., R. Havercamp, J. L. Starr, C. Fuentes, R. S. Malik, S. Kumar and R. K. Malik. 1990. Note - Maximal Capillary Rise Flux as a Function of Height from the Water Table. Soil Sci. 150:896-898.

Petrucci, R. H. 1985. General Chemistry - Principles and Modern Applications. 4th Edition. Macmillan Publishing Company, New York.

Philip, J. R. 1957. The Theory of Infiltration: 1. The Infiltration Equation and its Solution. Soil Sci. 83:345-357.

Philip, J. R. 1964. Similarity Hypothesis for Capillary Hysteresis in Porous Materials. J. Geophys. Res. 69:1553-1562.

Philip, J. R. 1991. Horizontal Redistribution with Capillary Hysteresis. Water Res. Research. 27:1459-1469.

Potter, M. C. and D. C. Wiggert. 1991. Mechanics of Fluids. Prentice-Hall, New Jersey.

Richards, L. A. 1931. Capillary Conduction of Liquids through Porous Mediums. Physics 1:318-333.

Singer, M. J. and D. N. Munns. 1987. Soils - An Introduction. Macmillan Publishing Company, New York.

Stakman, W. P. 1966. The Relation Between Particle Size, Pore Size and Hydraulic Conductivity of Sand Separates. UNESCO Symposium on Water in the Unsaturated Zone. II:373-383.

Suter, M. 1964. Effects of Voids and Permeability on Ground-Water Flow Condition. Waterworks and Wastes Engineering. 1:41.45.

Swartzendruber, D., M. F. DeBoodt and D. Kirkham. 1954. Capillary Intake Rate of Water and Soil Structure. Soil Sci. Soc. Am. Proc. 18:1-7.

Swartzendruber, D. 1969. The Flow of Water in Unsaturated Soils. In Flow Through Porous Media. Ed. R. J. M. De Wiest. Academic Press, New York. 215-292.

Terzaghi, K. and R. B. Peck. 1967. Soil Mechanics in Engineering Practice. 2nd Edition. John Wiley and Sons, Inc., New York.

USEPA. 1980. Design Manual - Onsite Wastewater Treatment and Disposal Systems. Office of Research and Development, Municipal Enviro. Research Lab. Cincinnati, Ohio. USEPA 625/1-80-012.

Wadsworth, H. A. and A. Smith. 1926. Some Observations upon the Effect of the Size of the Container upon the Capillary Rise of Water through Soil Columns. Soil Sci. 22:199-211.

Wind, G. P. 1966. Capillary Conductivity Data Estimated by a Simple Method. UNESCO Symposium on Water in the Unsaturated Zone. 181-191.

Wladitchensky, S. A. 1966. Moisture Content and Hydrophility as Related to the Water Capillary Rise in Soils. UNESCO Symposium on Water in the Unsaturated Zone. 360-365.